Latin American Journal of Aquatic Research, 52(1): 119-149, 2024
DOI: 10.3856/vol52-issue1-fulltext-2991

Research Article

Transcriptome characterization of *Pocillopora grandis* transplanted into reefs with different health conditions: potential stress indicators at the holobiont level

Oscar E. Juárez[1], Blanca Morales-Guerrero[1], Marco A. Liñán-Cabello[2]
Eugenio Carpizo-Ituarte[3], Erick Delgadillo-Nuño[1]
Manuel Alejandro Delgadillo-Nuño[1,3,5], Ricardo Gómez-Reyes[4]
Claudia Ventura-López[1], Rafael A. Cabral-Tena[5] & Clara E. Galindo-Sánchez[1]
[1]Laboratorio de Genómica Funcional, Departamento de Biotecnología Marina, Centro de Investigación Científica y de Educación Superior de Ensenada, Ensenada, Baja California, México
[2]Facultad de Ciencias Marinas, Universidad de Colima, Manzanillo, Colima, México
[3]Laboratorio de Ecología y Biología del Desarrollo (EcoDel), Instituto de Investigaciones Oceanológicas Universidad Autónoma de Baja California
Ensenada, Baja California, México
[4]Instituto de Investigaciones Oceanológicas (IIO)
Universidad Autónoma de Baja California, Ensenada, Baja California, México
[5]Departamento de Ecología Marina, Centro de Investigación Científica y de Educación Superior de Ensenada, Ensenada, Baja California, México
Corresponding author: Clara E. Galindo-Sánchez (cgalindo@cicese.mx)

ABSTRACT. Understanding the potential of coral to adapt to environmental stressors that cause coral bleaching is urgent. The molecular responses of the coral holobiont to such stress conditions determine the success of symbiosis. Therefore, by characterizing molecular stress responses at the holobiont level, we can develop better tools to diagnose its health and resilience. However, only some genomic-scale resources are available for reef-building corals from the Eastern Tropical Pacific. This study aimed to perform a transcriptomic characterization of the *Pocillopora grandis* holobiont following transplantation into environments with different health conditions in Colima, Mexico. Healthy specimens of two color morphotypes (green and brown) were collected in Carrizales, a reef in good condition. Coral fragments from the two morphotypes were relocated within the source location (local transplant stress). In contrast, similar fragments were translocated into another reef with a poorer health state, La Boquita. After 24 h, the transplanted fragments were collected, and RNA-seq was performed with the Illumina system. *De novo* transcriptome assembly, functional annotation, identification of co-expression modules, and enrichment analysis of molecular pathways were performed. The analysis of rRNA LSU, rRNA SSU, and COI sequences confirmed the coral species, whereas analysis of *Rubisco*, *psbA*, and *psaA* transcripts revealed that the dominant endosymbiont was *Durusdinium* sp. Gene expression patterns observed across samples suggest that the transplantation to a reef with a poorer state of health affected processes such as photosynthesis, calcium homeostasis, and immune response. The transcriptomic indicators proposed here are valuable for further studies examining the adaptation of *Pocillopora* corals to global changes.

Keywords: *Pocillopora grandis*; coral holobiont; symbiosis; stress indicators; co-expression; RNA-Seq

Associate Editor: Hugo Montaldo

INTRODUCTION

Various stressors have played a major role in the worldwide decline of coral reefs through accelerated industrialization, urbanization, agriculture, and climate change, including increasing sea surface temperatures, pollution, and diseases (Suggett & Smith 2020, Donovan et al. 2021). Corals attempt to acclimate to such environmental stresses by eliciting different molecular mechanisms that alter gene transcription in the short term (Onyango et al. 2021). At the holobiont level, however, this response is particularly complex due to the symbiotic associations between corals, endosymbionts, and microbial communities (Thurber et al. 2009). Therefore, the potential effects, responses, and resilience can vary across species and different environmental conditions (Maor-Landaw et al. 2014, Bay & Palumbi 2015, 2017, Arotsker et al. 2016, Thomas et al. 2019, Studivan & Voss 2020, Varasteh et al. 2021).

In the past decade, numerous genomic- and transcriptomic-scale resources, most notably RNA-sequencing, have emerged for the study of these complex processes in scleractinian corals (Shinzato et al. 2014a,b, Bay & Palumbi 2015, Bertucci et al. 2015, Mohamed et al. 2016, Zhang et al. 2017, 2018, Yuyama et al. 2018, Ryu et al. 2019, Liu et al. 2021, Brener-Raffalli et al. 2022, Yoshioka et al. 2022); and have proven to be useful in assessing specific responses of holobionts to environmental stress (Libro et al. 2013, Pinzón et al. 2015, Anderson et al. 2016, Aguilar et al. 2017, Hou et al. 2018, Helmkampf et al. 2019, Takagi et al. 2020, Ishibashi et al. 2021, Zhang et al. 2022). Genomic and transcriptomic resources also allow for a better understanding of the holobiont capacity of resistance, acclimatization, and resilience to climate change conditions (Moya et al. 2012, Barshis et al. 2013, Maor-Landaw et al. 2014, Seneca & Palumbi 2015, Davies et al. 2016, González-Pech et al. 2017, Kirk et al. 2018, Cooke et al. 2020, Savary et al. 2021).

The -omics information is growing for some widely distributed and ecologically important *Pocillopora* corals, which present high diversity and plasticity. Although the majority of studies are focused primarily on two species, *P. damicornis* (Vidal-Dupiol et al. 2013, 2014, Mayfield et al. 2014, Yuan et al. 2017, Zhou et al. 2017, Zhang et al. 2018, Guo et al. 2021, Li et al. 2021,) and *P. acuta* (Poquita-Du et al. 2019, 2020, Chuang & Mitarai 2020, 2021), recent projects like the Tara Pacific program and expedition (Planes et al. 2019, Armstrong et al. 2023) have expanded this approach on other pocilloporid species. However, genomic and transcriptomic studies are particularly lacking for the Tropical Eastern Pacific corals (Johnston et al. 2017, 2022, Armstrong et al. 2023).

The antler coral *Pocillopora grandis* Dana (1846), previously described as its junior synonym *Pocillopora eydouxi* (Schmidt-Roach et al. 2014, Claar et al. 2020), is one of the main reef-building corals in the Eastern Pacific (Pinzón & Lajeunesse 2011, Pinzón et al. 2013, Armstrong et al. 2023). This species is characterized by an extremely high phenotypic plasticity, reflected in the display of different color and skeletal morphotypes (Pinzón et al. 2013, Schmidt-Roach et al. 2014, Paz-García et al. 2015, Gélin et al. 2017, Johnston et al. 2017, Chiazzari et al. 2019). This study aims to characterize the transcriptome of this important species following its transplantation into different environments, emphasizing stress-response pathways at the holobiont level. In the differential gene expression analysis, we also compared the short-term transcriptomic response of holobionts to transplantation into reefs with different environmental conditions. The newly assembled transcriptome will be a valuable resource for further studies on the biological processes underlying corals' potential adaptation and resilience to global changes.

MATERIALS AND METHODS

Study area

The study area included two sites from the Tropical Eastern Pacific in Colima, Mexico. The Carrizales coral community (19°05'53"N, 104°26'11"W) was the original location of the coral colonies analyzed. Due to its high biodiversity value, this coral reef is cataloged as a "Priority Marine Area" by the Mexican National Commission for the Knowledge and Use of Biodiversity (CONABIO, by its Spanish acronym). In general, this area is considered to have a minimal impact by anthropogenic activity and is not exposed to excessive terrestrial runoff (Liñán-Cabello & Michel-Morfin 2018, Cadena-Estrada et al. 2019). Subsequently, coral fragments were transplanted (details in the section below) into a different reef located 7 km away, called La Boquita (19°06'10"N, 104°23'46"W). This reef community comprises coral patches that cover an area of 3876.2 m^2, extending from the surface to a depth of 3.5 m (Liñán-Cabello et al. 2008). This community is under a variety of stressors, including contamination and higher turbidity (Liñán-Cabello et al. 2016, Ostria-Hernández et al. 2022), which are related to its proximity (~250 m) to the tourist beach also called La Boquita (Liñán-Cabello et al. 2008,

Hernández-López et al. 2020) and an artificial channel that flows from the Juluapan Lagoon into the coral reef (Suppl. Fig. S1).

We considered the general health condition as the main environmental difference between locations (transplant environment), being better for Carrizales than for La Boquita. Moreover, at La Boquita, besides the high anthropogenic impacts, there is a continuous process of habitat loss and coral bleaching (Liñán-Cabello et al. 2016, Liñán-Cabello & Michel-Morfin 2018). However, given the lack of *in situ* measurements of environmental parameters, we used historical oceanographic data to demonstrate that the average water quality between these reefs is different. Satellite image data registered monthly and averaged for an area of 4 km^2 from 2002 to 2022 was obtained from the MODIS Aqua sensor (https://giovanni.gsfc.nasa.gov/). The diffuse attenuation coefficient at 490 nm (Kd490), chlorophyll-*a* (Chl-*a*), and particulate organic carbon (POC) were compared between both locations, including 240 measurements per parameter by implementing Mann-Whitney tests since data failed the normality (Shapiro-Wilk) test. These historical water quality parameters were used as an approximation for turbidity on each reef (Suppl. Fig. S2). During our sampling, SCUBA divers noticed that coral patches were scarce in La Boquita, and only the brown morphotype was observed.

Sampling and coral transplantations

Coral fragments of 10-13 cm from two colonies of the branching coral *P. grandis* of each color morphotype (i.e. green and brown, Suppl. Fig. S3), with a healthy appearance and no signs of bleaching or any other abnormal conditions according to the *CoralWatch* coloration scale (Siebeck et al. 2008), were collected at 2 m in depth at 09:00 h from the Carrizales reef in April 2017. Both colonies were fractionated and immediately relocated within the same location (local transplantation). All specimens were placed with the same orientation to the sea surface, as in their place of origin, with no more than 20 m between them. Corals show quick transcriptomic responses to physical stress, such as transplantations, which are more evident within the first day after coral fragmentation (Lock et al. 2022). Therefore, to capture rapid gene expression changes induced by transplantation, we adopted a one-day timeframe for transcriptomic analysis. Two samples of the relocated colonies of each color morphotype were taken the next day at zenith (14:00 h) and stored in 10 mL of RNAlater (Sigma-Aldrich, St. Louis, MO, USA) solution.

Four additional fragments-two from the green morphotype and two from the brown-were placed in a plastic container with oxygenated seawater under similar conditions of light and temperature and moved using a small boat to La Boquita, where they were transplanted with the same specifications as in Carrizales. The next day, two samples of each color morphotype were taken at the zenith time and stored in 10 mL of RNAlater (Sigma-Aldrich, St. Louis, MO, USA) solution.

RNA-seq

RNA extraction was performed following the protocol of Anderson et al. (2016) from two green and two brown coral fragments relocated in Carrizales and two green and two brown ones moved to La Boquita. From each sample, 100 mg of tissue was homogenized with TRI Reagent (SIGMA, St. Louis, MO, USA) and 100 mg of glass beads 425-600 µm (SIGMA, St. Louis, MO, USA) as a disruptive matrix in a FastPrep-24 Instrument (MP Biomedicals, Solon, OH, USA). After homogenization, 1-5 µL of HCl 6M was added to each sample, and RNA was extracted following the TRI Reagent protocol. According to the manufacturer's instructions, DNA was eliminated using purification columns (RNeasy Plus Mini Kit, Qiagen). The RNA was quantified with a NanoDrop 2000 spectrophotometer (Thermo Scientific), and its integrity was assessed using the Bioanalyzer Instrument 2100 (Agilent Technologies). Four sequencing libraries were prepared: Carrizales green (CG), Carrizales brown (CB), La Boquita green (BG), and La Boquita brown (BB); each library included equal amounts of RNA from two different colonies. The libraries were prepared using the TruSeq RNA Library Prep Kit v2, and sequencing was conducted in the HiSeq 2500 (Illumina) system. Library preparation and sequencing were performed at the Center for Aquaculture Technologies (San Diego, CA, USA).

***De novo* transcriptome assembly**

The quality of the reads was assessed with FastQC software (https://www.Bioinformatics.babraham.ac.uk/projects/fastqc/). The reads with averaged Phred33 score below 25 (5-base sliding window), sequencing adapters, short reads below 36 bp long, and 5-base heads from each read were removed with Trimmomatic v0.35 (Bolger et al. 2014). Transcriptome assembly and downstream analyses were performed at the holobiont level (including transcripts of corals and symbionts) considering the emerging evidence of the metabolic complementation among the community of metazoans,

protists, and microbes associated with scleractinian corals (Thurber et al. 2009, Thompson et al. 2015). The reference transcriptome was assembled *de novo* using Trinity v2.4.0 with default parameters (Grabherr et al. 2011), including all the libraries. Using Transrate software (Smith-Unna et al. 2016), the assembled contigs' quality was assessed to identify and remove possible artifacts or misassembled sequences. The resulting high-quality assembly, together with the raw sequence read archives (SRA), were deposited in the National Center for Biotechnology Information (NCBI) databases (GenBank Bio Project: PRJNA552592; Bio samples: SAMN12213361-SAMN12213364; TSA accession: GJZD00000000). Transcriptome completeness was assessed by the benchmarking universal single-copy orthologs (BUSCO) approach using as reference the metazoan_odb10 and alveolata_odb10 databases of BUSCO v5.3.2 with default parameters (Simão et al. 2015).

Transcriptome annotation and molecular identification of coral and endosymbiont species

Transcripts and coding sequences were annotated following the Trinotate pipeline v3.2.2 (Bryant et al. 2017) using updated databases (May 2022). The coral species was confirmed by analyzing transcript sequences annotated as cytochrome *c* oxidase subunit 1 (TRINITY_DN98458_c0_g1_i1), rRNA large subunit (TRINITY_DN68564_c0_g1_i1), and rRNA small subunit (TRINITY_DN3780_c0_g1_i1), showing blast hits with cnidarian species. The symbiont species were identified by analyzing transcript sequences annotated as ribulose-1,5 bisphosphate carboxylase/oxygenase (TRINITY_DN38466_c0_g4_i1), photosystem II protein D1 (TRINITY_DN39813_c1_g1_i1), and photosystem I P700 chlorophyll-*a* apoprotein A1 (TRINITY_DN32493_c0_g1_i1) showing blast hits with dinoflagellate species. These sequences were analyzed with a nucleotide BLAST (megablast option) against the NCBI nr/nt database at the BLAST website using default parameters (https://blast.ncbi.nlm.nih.gov/Blast.cgi).

Identification of gene clusters associated with stress responses

We used the protein BLAST hits (UniProt IDs) of translated coding sequences to perform functional enrichment analyses using the Database for Annotation, Visualization, and Integrated Discovery (DAVID v6.8) (Huang et al. 2009). Functions of animal-type gene products were analyzed using databases of animal models as background (human, mouse, zebrafish, and fly databases included in DAVID). In contrast, for the functions of plant-type gene products (belonging to the photosynthetic endosymbiont), the *Arabidopsis thaliana* model was used as background. The enrichment analysis was performed for gene ontology terms (FDR < 0.01, fold enrichment >2). The names of gene products from enriched processes related to "stress" were extracted and submitted to the STRING website (https://string-db.org/) to construct protein-protein interaction networks (Szklarczyk et al. 2015, 2017).

Cluster analysis for samples and transcripts

We used Bowtie2 (Langmead & Salzberg 2012) to map the reads from each library on the assembled transcriptome and RSEM (Li & Dewey 2011) to estimate the transcript abundance (transcripts per million, TPM). For sample clustering, a Pearson correlation was performed between sample pairs based on transcript abundances, and then samples were clustered by correlation values, followed by a principal component analysis. Analyses using default parameters were run following Perl and R scripts included in Trinity v2.8.5. For transcript clustering, the normalized transcript abundance matrix ($\log_2$ (TPM+1)) was filtered (counts per million > 1, sample frequency ≥ 2). A weighted signed network was then performed using the WGCNA R package (Langfelder & Horvath 2008) (soft-threshold = 29, method = Pearson). The trait association significance of the resulting clusters (here called modules) was calculated using an asymptotic student test ($P < 0.05$). Functional enrichment analysis for each module was performed based on transcript annotations from the EggNOG database ($P < 0.05$).

Differential gene expression analysis

Regardless of their color morphotype, the two samples from each location were grouped, and groups were compared to test the effect of the transplantation environment on gene expression. Likewise, an independent analysis was performed to test the effect of the color morphotype on gene expression, grouping samples per color regardless of their location. In both cases, samples within each group were used as replicates. The R package DESeq2 (Love et al. 2014) was implemented to calculate dispersion values and identify differentially expressed genes (DEGs) between the groups (false discovery rate < 0.01, fold change > 2, TPM > 1). Gene ontology annotations of DEGs were extracted and analyzed to obtain enriched ontology terms (biological process, molecular function, and cellular component) for each condition using the

GOseq package (Young et al. 2010) on R ($P < 0.05$). The bioinformatics pipeline was performed following Perl and R scripts included in Trinity v2.8.5. The top DEGs between Carrizales and La Boquita were reported as candidate genes to monitor this important species' response to environmental changes at the holobiont level.

RESULTS

De novo transcriptome assembly

The sequencing generated 18,800,784 ± 681,942 (mean ± standard deviation) paired reads per library with 101 bp in length and GC content between 50 and 60%. The 80 ± 0.1% of total reads survived the quality trimming. The assembly was filtered to remove artifacts and misassembled contigs. The resulting reference transcriptome consisted of 110,319 transcripts corresponding to 97,726 'Trinity genes', with a contig N50 of 1012 and an average contig length of 668.66 nucleotides. The analysis of transcriptome completeness showed that 77.3% (72.6% complete and 4.7% fragmented genes) of Alveolata orthologous genes were present in our assembly, whereas 71.6% (61.8% complete and 9.8% fragmented genes) of metazoan genes were represented (Table 1).

Table 1. Summary of the transcriptome assembly and annotation of *Pocillopora grandis* holobiont. nt: nucleotides; RNA-seq libraries of green and brown morphotypes from two reefs in the tropical Eastern Pacific (Colima, Mexico).

Reads passing the quality filter	120,335,509 (101 nt read length)
Number of putative genes	97,726
Number of transcripts	110,319
Average contig length	668.66 nt
N50	1,012 nt
Assembly GC%	47.33
BLASTp hits (UniProt database)	23,241
Transcriptome completeness	alvoelata database: 77.3% metazoan database: 71.6%

Molecular identification of coral and endosymbiont species

The analyzed metazoan genes (rRNA large subunit, rRNA small subunit, and COI) matched with *P. grandis* (senior synonym of *P. eydouxi* Milne Edwards, 1860) sequences with a similarity of 100-99.9%, the highest among other hits with pocilloporid sequences from GenBank. On the other hand, the photosynthetic genes (Rubisco, psbA, and psaA) showed higher similarity (96.07-96.61%) with sequences from *Durusdinium* sp. and *Symbiodynium* clade *D* (Suppl. Table S1). It is worth mentioning that *Durusdinium* sp. was formerly named *Symbiodinium* clade *D* (LaJeunesse et al. 2018).

Transcriptome annotation and identification of stress-related genes

Twenty-three thousand two hundred forty-one transcripts received blast hits against the UniProt database and gene ontology annotations. These annotations were used for enrichment analysis of gene ontology terms using animal model species as backgrounds (human, mouse, zebrafish, and fly). Significant enrichment was observed for stress-related processes such as the response to radiation (35 gene products), response to oxidative stress (34 gene products), and regulation of cell death (63 gene products), among others. In addition, a significant enrichment of stress-related processes was obtained using a photosynthetic model (*Arabidopsis thaliana*), including the response to salt stress (36 gene products), response to osmotic stress (22 gene products), response to water deprivation (20 gene products), response to light intensity (13 gene products) and plant-type hypersensitive response (7 gene products) among others. Stress-related genes were extracted, separating those enriched in the animal models from those enriched in the plant model. These two stress-related gene sets were analyzed to construct protein-protein interaction networks (Suppl. Figs. S4-S5). These interaction networks suggest that coral and endosymbiont cooperate in the stress-induced MAPK pathway. Some components of this pathway were present in the animal-type network, while others were in the plant-type network. As expected, the animal-type stress response was clearly distinguished by genes encoding hypoxia-inducible factors, TNF receptor-associated factors, and cyclin-dependent kinases. On the other hand, the plant-type stress response was characterized by genes encoding calcium-dependent protein kinases, calcium-binding proteins, calmodulins, and endoribonucleases.

Cluster analysis for samples and transcripts

In the cluster analysis, a dataset of 47,906 transcripts was split into ten co-expression modules. Transcripts from these modules were classified into biological processes such as genetic information processing (transcription, replication, and translation), cellular processes (defense mechanisms, post-translational modification, protein turnover, and chaperones), and metabolism (energy production, as well as carbohydrate, amino acid, and lipid metabolisms) (Fig. 1). Based on the trait association analysis, two modules, "turquoise" (17,567 transcripts) and "blue" (11,383

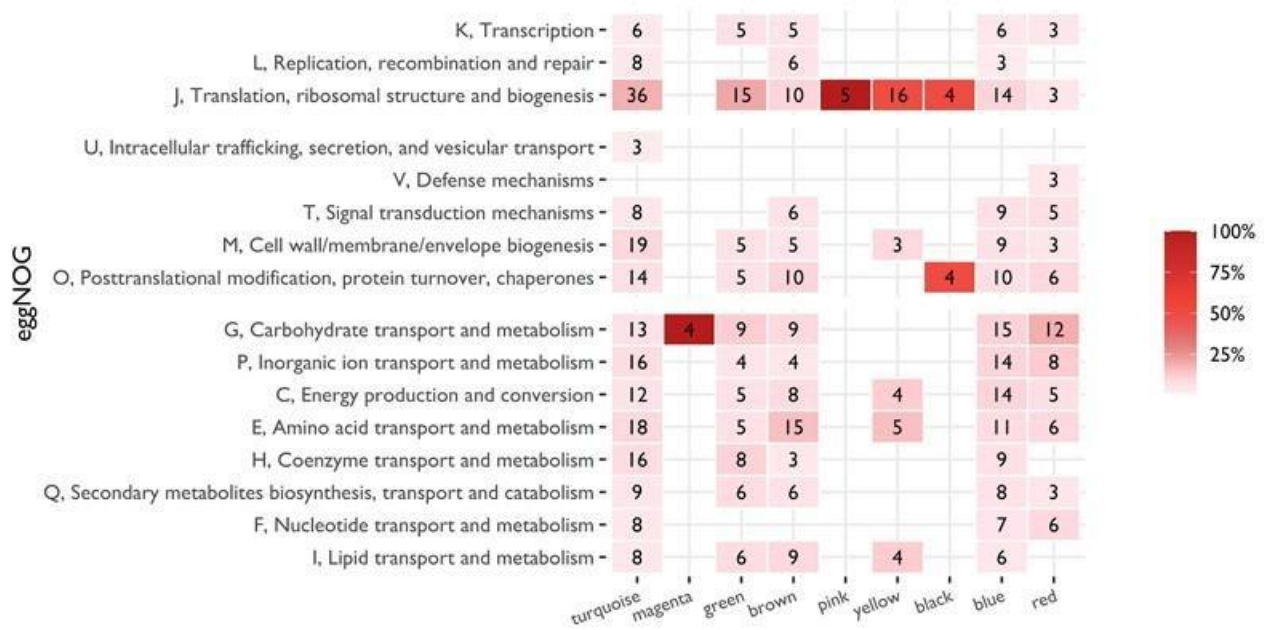

Figure 1. Functional enrichment for co-expression modules in the transcriptome of *Pocillopora grandis* after transplantation procedures. Modules were obtained based on transcript abundance across all RNA-seq samples. The number of transcripts within each eggNOG term is shown for each module. The eggNOG terms are categorized in genetic information processing (K, L, and J), cellular processes (U, V, T, M, and O), and metabolism (G, P, C, E, H, Q, F, and I). Only transcripts with known pathway classification were analyzed.

transcripts) showed opposite expression patterns. They were significantly associated with the transplantation environment (Fig. 2).

The blue module, significantly associated with La Boquita, included transcripts for glyceraldehyde-3-phosphate dehydrogenase 2, related to glucose regulation (Ugrankar et al. 2015); patatin-like phospholipase domain-containing protein 6, involved in lipid catabolic process (Zaccheo et al. 2004); 5'-methylthioadenosine/S-adenosylhomocysteine nucleosidase, which participates in methionine recycling and biosynthesis (Siu et al. 2008, 2011); protochlorophyllide-dependent translocon component 52, involved in protein transport (Bartsch et al. 2008), among other transcripts participating in transmembrane transport of nutrients and other metabolites.

The turquoise module, significantly associated with corals transplanted in Carrizales, included transcripts for polycystin-2, involved in the release of intracellular calcium (Koulen et al. 2005); phosphoenolpyruvate/phosphate translocator 2 and UDP-N-acetylglucosamine transporter, related to carbohydrate transport (Nozawa et al. 2007, Toscanini et al. 2019); cobalamin trafficking protein CblD, participating in vitamin biosynthesis (Jusufi et al. 2014); lipoxygenase 1 and acyl-coenzyme A thioesterase 13, involved in the biosynthesis and regulation of fatty acid levels (Wei et al. 2009, Liu et al. 2019); START domain-containing protein 10, associated with lipid transport (Olayioye et al. 2005); and several transcripts involved in intracellular protein transport.

The sample cluster analysis showed that the transplantation environment was the main factor affecting gene expression patterns. Both samples from Carrizales were grouped; likewise, both samples from La Boquita formed another group (Fig. 3). According to the PCA, component "one" arranged samples by location (59.42% of variation), component "two" arranged samples by color (29.99% of variation), and component "three" arranged samples by the interaction of factors (10.59% of variation) (Fig. 4).

Differential gene expression analysis

In comparing locations, 2514 transcripts were upregulated in La Boquita, whereas only 161 were upregulated in Carrizales. On the other hand, in the comparison between color morphotypes, 211 transcripts showed higher expression in the brown. In comparison, 76 showed higher expression in the green morphotype (Fig. 5). We obtained significant enrich-

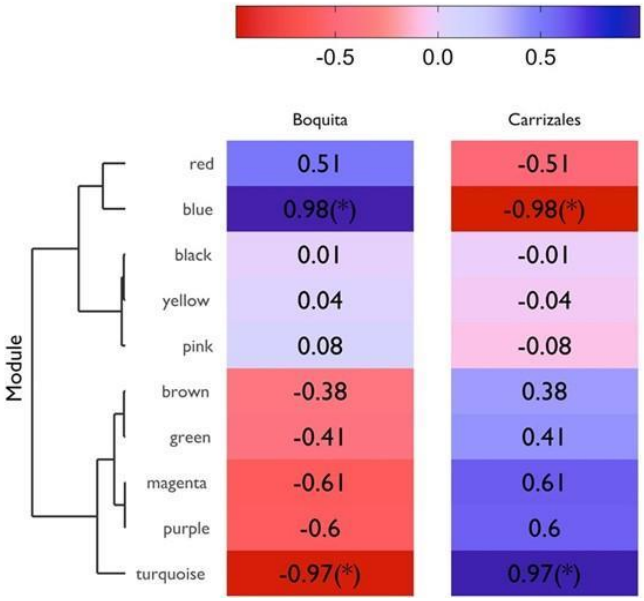

Figure 2. Trait association analysis (transplantation environment) for co-expression modules detected in the *Pocillopora grandis* transcriptome. The modules "blue" and "turquoise" showed significant association with transplantation environment (*). The color shades represent the co-expression significance of the modules (dark red: no significant; dark blue: highly significant). The "blue" module was significantly co-expressed at La Boquita, while the "turquoise" was significantly co-expressed at Carrizales.

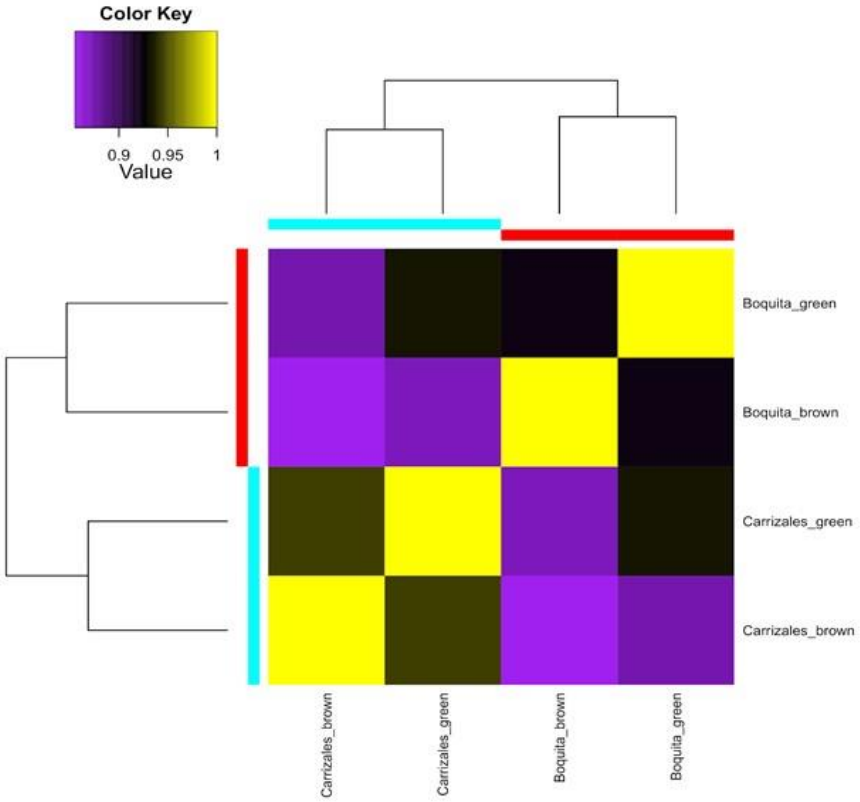

Figure 3. Correlation heatmap and clustering of *Pocillopora grandis* holobiont samples from green and brown morphotypes transplanted into Carrizales and La Boquita reefs in Colima, Mexico. Samples from Carrizales are marked with blue bars, and samples from La Boquita are marked with red bars (on left and top sides). Correlation is based on transcript abundance (counts per million).

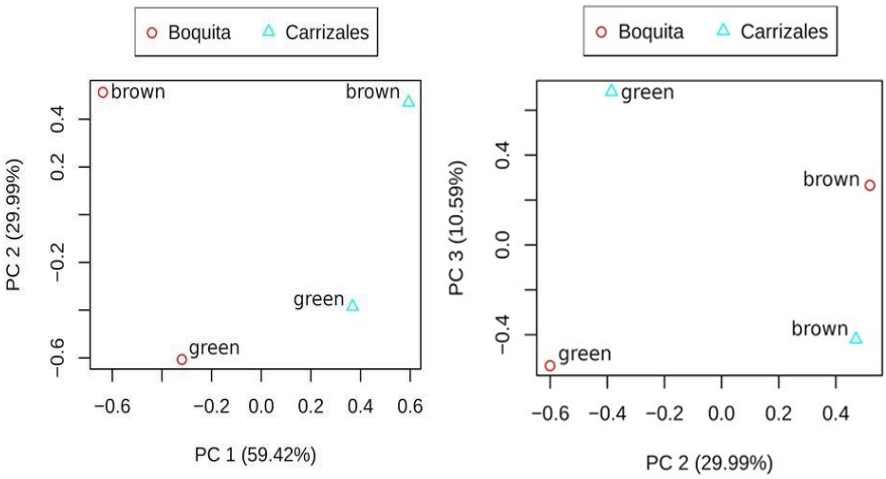

Figure 4. Principal component analysis for *Pocillopora grandis* holobiont samples from different color morphotypes and transplant environments. Analysis based on transcript abundance across samples (counts per million).

ment of gene ontology terms for every condition in both comparisons: in Carrizales, upregulated genes enriched terms such as the photosynthesis dark reaction, donor selection, and long-chain fatty acid catabolic process. In La Boquita, photosynthesis light-harvesting, protein-chromophore linkage, and positive regulation of stress-activated MAPK cascade are among the top enriched GO terms. On the other hand, in the comparison between color morphotypes, genes upregulated in the brown morphotype enriched GO terms such as muscle cell fate specification, negative regulation of cellular senescence, and apolipoprotein A-I-mediated signaling pathway, while genes upregulated in the green morphotype enriched GO terms including propionate catabolic process, glycerol biosynthetic process from pyruvate, and biolumi-nescence (Suppl. Table S2). Interestingly, the bioluminescence GO term was enriched due to a higher expression of the green fluorescent protein gene (GFP) in the green morphotypes compared to the brown.

Potential stress markers

We selected the top 30 DEGs (based on statistical significance) between the locations as candidate genes for monitoring gene expression changes associated with environmental changes. Historical remote-sensing data showed higher productivity (inferred from Chl-*a* concentration) and turbidity (Kd490 coefficient) and lower water quality (higher POC concentration) in La Boquita compared to Carrizales (Suppl. Fig. S2). Interestingly, many of the top DEGs belong to pathways from photosynthesis, calcium homeostasis, ion transport, apoptosis, and oxidation-reduction processes (Fig. 6). An extended list of DEGs between

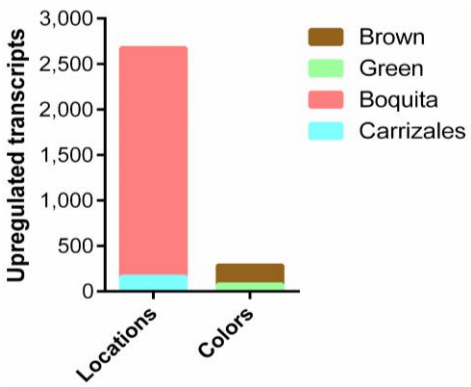

Figure 5. The number of upregulated transcripts in pairwise comparisons between color morphotypes and transplant locations of *Pocillopora grandis* holobiont from Colima, México. Upregulated transcripts at La Boquita highly exceed those at Carrizales and those between green and brown morphotypes.

La Boquita and Carrizales including transcript IDs and normalized gene expression values (counts per million) is provided as Supplementary Material (Suppl. Table S3).

DISCUSSION

Complementary transcriptomic response of coral and endosymbiont to transplantations

Although transplantations, along with nursery growth, are considered essential to coral restoration, these are stressful events for the coral holobiont, characterized by physical fragmentation and outplanting (Ferse et al. 2021, Cook et al. 2022, Lock et al. 2022). Our study used local and remote transplantation procedures to

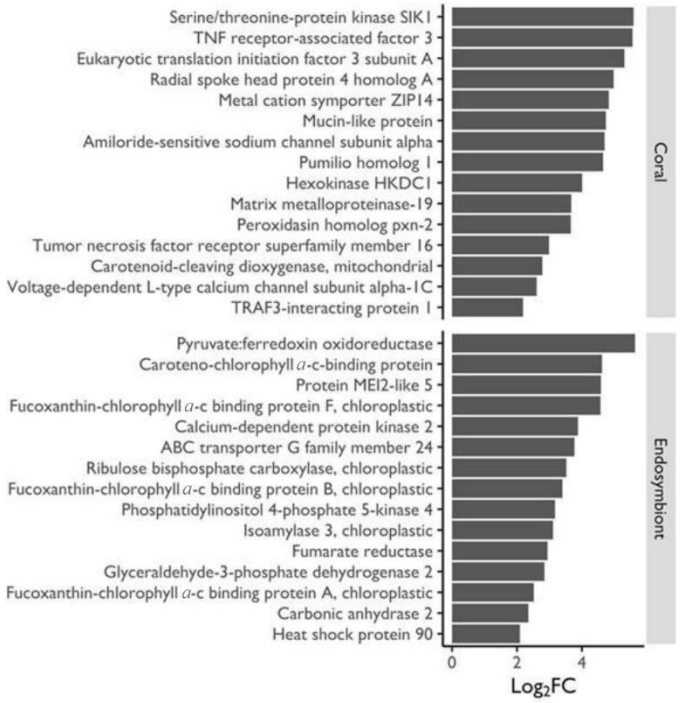

Figure 6. Top 30 candidate marker genes for monitoring the response to environmental changes in the holobiont of *Pocillopora grandis.* These top-DEGs were all upregulated in La Boquita reef (unhealthy) *vs.* Carrizales reef (healthy). Transcript origin was classified as "coral" if the sequence showed BLAST hits with metazoan genes and "endosymbiont" if the hits corresponded to other (non-metazoan) eukaryotic genes.

induce stress responses on the entire "coral holobiont" and described such responses at the molecular level. Our successful experiment allowed us to detect both animal- and plant-type stress responses in the *P. grandis* holobiont, which presumably correspond to coral and endosymbiont. Interestingly, these animal and plant-type responses seem to be complementary. For example, we found both animal- and plant-like genes participating in the stress-activated MAPK cascade. A fraction of coral and endosymbiont transcriptomes was presumably absent or silenced-as suggested by the "incompleteness" observed in our assembled holobiont transcriptome-possibly due to symbiosis. More than 20% of both metazoan and alveolata orthologous genes were missing. The obligate symbiosis between corals and Symbiodiniaceae and its coevolution may partly explain this "incompleteness" of our holobiont transcriptome (Thompson et al. 2015).

In this regard, we also identified ten transcript co-expression modules in the holobiont transcriptome, which were enriched by diverse nutrient biochemical pathways like glucose regulation, amino acid recycling and biosynthesis, regulation of fatty acid levels, vitamin biosynthesis, calcium homeostasis, and transport of proteins and other metabolites, including both animal- and plant-type transcripts. From this result, we can hypothesize a complementary gene expression between coral hosts and their endosymbionts, where the host's lack of essential nutrients and metabolites may be compensated with those synthesized by the endosymbionts and vice versa.

A previous study found similar evidence of complementarity in the amino acid metabolism between simultaneously sequenced transcriptomes of *Porites australiensis* and its *Cladocopium* sp. symbionts (Shinzato et al. 2014a). Biochemical complementarity has also been found in the genomes of many *Acropora* corals and their Symbiodiniacea endosymbionts (Shinzato et al. 2011, 2021). Moreover, the *Fugacium kawagutii* genome contains the complete biosynthesis pathways of all the essential amino acids *Acropora digitifera* cannot produce. Still, it lacks the genes of the four major photoprotector mycosporine-like amino acids (MAAs) found in *A. digitifera* (Lin et al. 2015). Additionally, Symbiodiniaceae species could potentially regulate target genes involved in photosynthesis, stress response, and symbiosis in both symbiont and coral genomes. Interestingly, these genes are subject to RNA edition and differential regulation by microRNAs under different heat, light, and nutrient conditions (Lin et al. 2015, Zhu et al. 2022b).

Our newly assembled transcriptome opens the door for further studies into cross-organism gene complement and gene co-expression analysis of the *P. grandis* holobiont better to understand its symbiotic interactions and responses to the environment.

Holobiont response to distinct transplantation environments

The transplantation environment was the main factor influencing the observed gene expression patterns across the samples, affecting biological processes including photosynthesis, antioxidant response, apoptosis, immune response, and calcification. In addition, the transplantation environment was significantly associated with two co-expression modules, the "blue" (11,383 transcripts) and the "turquoise" (17,567 transcripts). The "blue" co-expression module association was significant in La Boquita, while the "turquoise" was significant in Carrizales.

Both "blue" and "turquoise" modules included several transcripts involved in nutrient biochemical pathways; however, these pathways reflect that holobionts used nutriments distinctly in each reef, independently of their color morphotype. For example, co-expressed transcripts in La Boquita were involved in lipid catabolism, amino acid recycling, and transmembrane transport of proteins and other metabolites. While in Carrizales, the co-expressed transcripts were associated with calcium release, fatty acid regulation and biosynthesis, intracellular protein transport, and vitamin biosynthesis.

Interestingly, the protochlorophyllide-dependent translocon component 52, a gene downregulated by light (Bartsch et al. 2008), showed higher expression in La Boquita and was a component of the "blue" module, with significant co-expression in La Boquita, suggesting that lower light intensity or quality in La Boquita (compared to the original location, Carrizales) could induce the expression of this gene and, possibly, the expression of the whole module. On the other hand, the "turquoise" module co-expressed in Carrizales could be associated with a better health condition of the holobionts since this module was mainly associated with biosynthetic pathways. However, it must be further investigated if these co-expressed genes could be used as indicators of the health status of this and other tropical coral species.

In this regard, La Boquita entails a greater challenge for the corals due to stressors, such as higher sedimentation and turbidity, contaminants, and potentially infectious organisms (Liñán-Cabello et al. 2008, 2016). Besides, high values of ammonium, Chl-*a*, and extinction coefficient were reported previously at this site (Ostria-Hernández et al. 2022). These conditions seem to affect light penetration since the expression levels of *psbA* were lower than those detected for Carrizales. By contrast, the FCP complex showed multiple isoforms and higher expression in La Boquita than Carrizales for both morphotypes. Although the FCP complex is upregulated in various stress conditions (Hwang et al. 2008, Nymark et al. 2009, Dittami et al. 2010, Park et al. 2010, Strychar & Sammarco 2011), in this case, the complex could be functioning as a light-harvesting system enhancing photosynthesis under dim-light (Ishihara et al. 2015). This response seems to be coupled with the upregulation of carbonic anhydrase and rubisco genes, which are essential for carbon fixation during photosynthesis (Tsuzuki & Miyachi 1989, Badger & Price 1994, Badger 2003, Nishiyama et al. 2006, Venn et al. 2006, DiMario et al. 2018). In the present study, transcripts upregulated in La Boquita annotated as carbonic anhydrase 2 and ribulose biphosphate carboxylase (chloroplastic) showed blast hits with dinoflagellate species, suggesting that the upregulation of these genes occurred in the photosynthetic endosymbiont.

Another vital process in the physiology of corals is calcification (Reyes-Bermudez et al. 2009, Moya et al. 2012, Gutner-Hoch et al. 2017, Ross et al. 2022). The process is highly dependent on water quality and chemistry (Erez et al. 2011); therefore, it is strongly affected by environmental changes (Moya et al. 2012, Ross et al. 2022). In the present study, genes encoding galaxins and collagen variants, which participate in calcification (Reyes-Bermudez et al. 2009, Gutner-Hoch et al. 2017), showed an upregulation after coral transplantation to La Boquita that could reflect a strong effort of coral holobionts to compensate for the effect of stressful conditions on the skeletal morphology (Paz-García et al. 2015). An increase in linear skeletal extension has been observed from corals in sediment-impacted environments (Carricart-Ganivet & Merino 2001), presumably to reduce the risk of sediment burial and enhance light capture in turbid environments (Ng et al. 2019). In this regard, a previous study found larger skeletons in *Pocillopora* from La Boquita than those from the Carrizales reef (Delgadillo-Nuño et al. 2017), which supports our results.

Extracting corals from their original colonies and transplantation into a different environment could stimulate the expression of wound healing genes, such as those encoding matrix metalloproteinases (MMP) (Wright et al. 2015). We found significant overex-

pression of the *MMP19* gene in holobionts transplanted to La Boquita. In addition, genes encoding the mucin-like protein were conspicuous at this location. This protein participates in mucus secretion, part of the primary defense barrier against desiccation and infection (Jatkar et al. 2010). It is linked to immune protein activity (Fuess et al. 2016).

Besides the great stress that relocation to La Boquita caused the corals, 24 species of bacteria were previously found in *Pocillopora* sp. from this location (Laurel-Sandoval 2014). Among the bacteria, authors detected *Serratia*, an indicator of anthropogenic pollution (Patterson et al. 2002). A recent study also found a high relative bacterial abundance of the Planctomycetaceae and Pseudomonadaceae families in *Pocillopora* spp. near La Boquita (Ostria-Hernández et al. 2022). A high abundance of these bacteria has been associated with eutrophic environments and diseased corals (Sunagawa et al. 2009, Roder et al. 2014, Zhu et al. 2022a), which may explain the high expression of immune response genes detected at La Boquita in this study.

A bacterial challenge may be occurring after transplantation in both morphotypes linked to the cut and exposed tissue since the upregulation of genes related to antimicrobial defense pathways such as the tumor necrosis factor (TNF) pathway was detected (Palmer & Traylor-Knowles 2012, Pinzón et al. 2015). Although TNFs are well-known mediators of the cellular death pathway (Quistad et al. 2014), they are also important signal transducers mediating corals' immune system response (Libro et al. 2013, Anderson et al. 2016). The *TRAF3* gene was also upregulated at La Boquita. In previous studies, this gene and TRAF6 were upregulated after coral infections (Libro et al. 2013, Anderson et al. 2016). Moreover, the overexpression of toll-like receptors (TLRs) and integrins, which are related to immune recognition (Palmer & Traylor-Knowles 2012, Anderson et al. 2016), has been reported in those infections (Libro et al. 2013). Integrin genes such as *TIP* and *ITB1* have been reported to activate the phagocytic response (Palmer & Traylor-Knowles 2012). This set of immune genes showed higher expression at La Boquita in both morphotypes.

Metabolic processes are among the most affected during diverse stress conditions (Starcevic et al. 2010, Vidal-Dupiol et al. 2013, 2014, Pinzón et al. 2015). In our experiment, a wide variety of transcripts related to mitochondrial energy production were upregulated at La Boquita, indicating that stress response processes demand high amounts of energy. Interestingly, two co-expression modules with opposite expression patterns were associated with the transplantation environment. These were enriched with multiple metabolic processes, including energy production and conversion.

Differential expression of the green fluorescent protein gene

Among the genes with a higher difference in expression between the green and brown morphotypes was the *GFP*. The green morphotype showed the highest levels for this gene. The cnidarian expresses the *GFP*, which leads to the protection of the green coral holobiont from oxidation (Palmer et al. 2009) and UV light (Aranda et al. 2011, Smith et al. 2013). This protein modulates sunlight wavelength, making it less harmful for the holobiont and suitable to be used by the endosymbiont photosystem (Salih et al. 2000, Dove et al. 2001, Alieva et al. 2008).

It is important to consider that the natural occurrence of the green morphotype was not observed in the La Boquita reef during the present study. In this regard, a previous study on pocilloporid species from the Carrizales reef suggested that *GFP* gene expression may depend on water quality, light quality, and light intensity (Delgadillo-Nuño et al. 2020). Therefore, the actual conditions of water and light in Carrizales favor the expression of this gene and the proliferation of green morphotypes. Interestingly, in a previous restoration study in the Carrizales reef, brown morphotypes showed a change in coloration towards the green morphotype after one year of restoration practices (Liñán-Cabello et al. 2011).

A comparative study of the health status of Carrizales and La Boquita reefs revealed an average sedimentation rate of 148 g month^{-1} in La Boquita while in Carrizales it was 11 g month^{-1} (Liñán-Cabello et al. 2008). In addition, during a restoration study of *Pocillopora* spp., dissolved inorganic nitrogen (DIN) and PO_4 were generally lower in Carrizales throughout the year (Muñiz-Anguiano et al. 2017). From this, we can hypothesize that in the La Boquita reef, higher sedimentation rates, turbidity, and pollution diminish both water and light quality (Liñán-Cabello et al. 2016), affecting the *GFP* expression and allowing only the development of brown colonies, which may indicate that the brown morphotype is more resilient to impacted environments. Further research is needed to test this hypothesis.

Limitations of the study and recommendations for further research

Due to funding constraints and sampling restrictions, we could not sequence individual samples. Alternatively, biological replicates of each condition were pooled before sequencing to obtain a biological average. DEGs were then obtained using stringent quality controls and statistical significance, including the inter-sample variation estimation. In addition, our report focused on transcripts passing a minimum abundance filter (counts per million >1) to increase the reliability of results and minimize the false discovery rate. Although the number of biological replicates sequenced was below that recommended in the literature (Williams et al. 2014, Honaas et al. 2016), the DEGs reported here represent potential transcriptomic indicators to monitor the response of the coral holobiont to environmental changes, and their efficiency must be tested at the population level.

Using corals from favorable sites (water quality and ecosystem health) to restore reefs damaged directly by human activity or indirectly via bleaching-related mortality still benefits those unfavorable sites (Barott et al. 2021). However, an additional recommendation is to follow up on the transcriptomic responses of holobionts at both transplantation sites for longer periods. In a previous study in the same reefs, following the same transplantation design (local transplantation in Carrizales *vs*. transplantations from Carrizales to La Boquita), the survival and growth of *Pocillopora* sp. corals were monitored for ten months. Although survival showed no significant differences between both transplantation sites, the growth in length and thickness were significantly higher in Carrizales (Islas-Peña et al. 2013). Besides, the development of bleaching-related mortality in transplanted corals depends on various factors, including the health condition and bleaching-resistance of individuals, environmental conditions of the new location, the success of the transplantation process itself, and natural or thermal stress-induced bleaching events (Sampayo et al. 2016, Muñiz-Anguiano et al. 2017, Barott et al. 2021). Therefore, it is important to assess the long-term transcriptomic responses of holobionts to these conditions to understand better the factors and molecular mechanisms favoring or limiting the growth and fitness of corals after transplantation procedures.

Funding details: this study was funded by the Centro de Investigación Científica y Educación Superior de Ensenada (CICESE, Baja California, México) grant N°682123 approved for GSCE and by the Consejo Nacional de Ciencia y Tecnología (CONACyT, Mexico), through the Basic Science grant N°181597, approved for CIE. Raw sequence read archives (SRA) were deposited in the National Center for Biotechnology Information (NCBI) databases (GenBank: PRJNA552592, SRA: SAMN12213361-SAMN12213364). The transcriptome assembly project has been deposited at DDBJ/EMBL/GenBank under accession GJZD00000000.

ACKNOWLEDGMENTS

The authors thank Maider Justel Diez for her support during sampling and laboratory procedures and Alexis Eduardo Trejo Estrada for his suggestions on satellite data analysis.

REFERENCES

Aguilar, C., Raina, J.B., Motti, C.A., Fôret, S., Hayward, D.C., Lapeyre, B., et al. 2017. Transcriptomic analysis of the response of *Acropora millepora* to hypo-osmotic stress provides insights into DMSP biosynthesis by corals. BMC Genomics, 18: 1-14. doi: 10.1186/s12864-017-3959-0

Alieva, N.O., Konzen, K.A., Field, S.F., Meleshkevitch, E.A., Hunt, M.E., Beltran-Ramirez, V., et al. 2008. Diversity and evolution of coral fluorescent proteins. Plos One, 3: e2680. doi: 10.1371/journal.pone.0002680

Anderson, D.A., Walz, M.E., Weil, E., Tonellato, P. & Smith, M.C. 2016. RNA-Seq of the Caribbean reef-building coral *Orbicella faveolata* (Scleractinia-Merulinidae) under bleaching and disease stress expands models of coral innate immunity. PeerJ, 2016: e1616. doi: 10.7717/peerj.1616

Aranda, M., Banaszak, A.T., Bayer, T., Luyten, J.R., Medina, M. & Voolstra, C.R. 2011. Differential sensitivity of coral larvae to natural levels of ultraviolet radiation during the onset of larval competence. Molecular Ecology, 20: 2955-2972. doi: 10.1111/j.1365-294X.2011.05153.x

Armstrong, E.J., Lê-Hoang, J., Carradec, Q., Aury, J.M., Noel, B., Hume, B.C., et al. 2023. Host transcriptomic plasticity and photosymbiotic fidelity underpin *Pocillopora* acclimatization across thermal regimes in the Pacific Ocean. Nature Communications, 14: 3056. doi: 10.1038/s41467-023-38610-6

Arotsker, L., Kramarsky-Winter, E., Ben-Dov, E. & Kushmaro, A. 2016. Microbial transcriptome profiling of black band disease in a Faviid coral during a seasonal disease peak. Diseases of Aquatic Organisms, 118: 77-89. doi: 10.3354/dao02952

Badger, M. 2003. The roles of carbonic anhydrases in photosynthetic CO_2 concentrating mechanisms. Photosynthesis Research, 77: 83-94. doi: 10.1023/A:1025821717773

Badger, M.R. & Price, G.D. 1994. The role of carbonic anhydrase in photosynthesis. Annual Review of Plant Physiology and Plant Molecular Biology, 45: 369-392. doi: 10.1146/annurev.pp.45.060194.002101

Barott, K.L., Huffmyer, A.S., Davidson, J.M., Lenz, E.A., Matsuda, S.B., Hancock, J.R., et al. 2021. Coral bleaching response is unaltered following acclimatization to reefs with distinct environmental conditions. Proceedings of the National Academy of Sciences, 118: e2025435118. doi: 10.1073/pnas.2025435118

Barshis, D.J., Ladner, J.T., Oliver, T.A., Seneca, F.O., Traylor-Knowles, N. & Palumbi, S.R. 2013. Genomic basis for coral resilience to climate change. Proceedings of the National Academy of Sciences of the United States of America, 110: 1387-1392. doi: 10.1073/pnas.1210224110

Bartsch, S., Monnet, J., Selbach, K., Quigley, F., Gray, J., von Wettstein, D., et al. 2008. Three thioredoxin targets in the inner envelope membrane of chloroplasts function in protein import and chlorophyll metabolism. Proceedings of the National Academy of Sciences of the United States of America, 105: 4933-4938. doi: 10.1073/pnas.0800378105

Bay, R.A. & Palumbi, S.R. 2015. Rapid acclimation ability mediated by transcriptome changes in reef-building corals. Genome Biology and Evolution, 7: 1602-1612. doi: 10.1093/gbe/evv085

Bay, R.A. & Palumbi, S.R. 2017. Transcriptome predictors of coral survival and growth in a highly variable environment. Ecology and Evolution, 7: 4794-4803. doi: 10.1002/ece3.2685

Bertucci, A., Forêt, S., Ball, E.E. & Miller, D.J. 2015. Transcriptomic differences between day and night in *Acropora millepora* provide new insights into metabolite exchange and light-enhanced calcification in corals. Molecular Ecology, 24: 4489-4504. doi: 10.1111/mec.13328

Bolger, A.M., Lohse, M. & Usadel, B. 2014. Trimmomatic: a flexible trimmer for Illumina sequence data. Bioinformatics, 30: 2114-2120. doi: 10.1093/bioinformatics/btu170

Brener-Raffalli, K., Vidal-Dupiol, J., Adjeroud, M., Rey, O., Romans, P., Bonhomme, F., et al. 2022. Gene expression plasticity and frontloading promote thermotolerance in *Pocillopora* corals. Peer Community Journal, 2: e13. doi: 10.24072/pcjournal.79

Bryant, D.M., Johnson, K., DiTommaso, T., Tickle, T., Couger, M.B., Payzin-Dogru, D., et al. 2017. A tissue-mapped axolotl de novo transcriptome enables identification of limb regeneration factors. Cell Reports, 18: 762-776. doi: 10.1016/j.celrep.2016.12.063

Cadena-Estrada, A., Ortega-Ortiz, C.D. & Liñán-Cabello, M.A. 2019. Cryptic fish associated with different substrates in two coastal reef communities of Colima, Mexico. Latin American Journal of Aquatic Research, 47: 318-330. doi: 10.3856/vol47-issue2-fulltext-12

Carricart-Ganivet, J.P. & Merino, M. 2001. Growth responses of the reef-building coral *Montastraea annularis* along a gradient of continental influence in the southern Gulf of Mexico. Bulletin of Marine Science, 68: 133-146.

Chiazzari, B., Magalon, H., Gélin, P. & Macdonald, A. 2019. Living on the edge: assessing the diversity of South African *Pocillopora* on the margins of the Southwestern Indian Ocean. Plos One, 14: e0220477. doi: 10.1371/journal.pone.0220477

Chuang, P.S. & Mitarai, S. 2020. Signaling pathways in the coral polyp bail-out response. Coral Reefs, 39: 1535-1548. doi: 10.1007/s00338-020-01983-x

Chuang, P.S. & Mitarai, S. 2021. Genetic changes involving the coral gastrovascular system support the transition between colonies and bailed-out polyps: evidence from a *Pocillopora acuta* transcriptome. BMC Genomics, 22: 1-12. doi: 10.1186/s12864-021-08026-x

Claar, D.C., Tietjen, K.L., Cox, K.D., Gates, R.D. & Baum, J.K. 2020. Chronic disturbance modulates symbiont (Symbiodiniaceae) beta diversity on a coral reef. Scientific Reports, 10: 1-13. doi: 10.1038/s41598-020-60929-z

Cook, N., Smith, A., Songcuan, A., Cassidy, D., Sartori, G. & McLeod, I. 2022. Lessons learned from small-scale coral outplanting intervention at a restoration site on the Great Barrier Reef. Ecological Management and Restoration, 23: 89-93. doi: 10.1111/emr.12547

Cooke, I., Ying, H., Forêt, S., Bongaerts, P., Strugnell, J.M., Simakov, O., et al. 2020. Genomic signatures in the coral holobiont reveal host adaptations driven by Holocene climate change and reef-specific symbionts. Science Advances, 6: 48. doi: 10.1126/sciadv.abc6318

Davies, S.W., Marchetti, A., Ries, J.B. & Castillo, K.D. 2016. Thermal and pCO_2 stress elicit divergent transcriptomic responses in a resilient coral. Frontiers in Marine Science, 3: 112. doi: 10.3389/fmars.2016.00112

Delgadillo-Nuño, M.A., Carpizo-Ituarte, E., Liñán-Cabello, M.A., Hérnandez-Ayón, J.M. & Olivos-Ortiz, A. 2017. Extensión y crecimiento esquelético del coral *Pocillopora verrucosa* en la costa de Colima, México. In: Paz, F., Torres, R. & Velázquez, A. (Eds.). Estado

Actual del Conocimiento del Ciclo del Carbono y sus Interacciones en México: Síntesis a 2017. Serie Síntesis Nacionales. Programa Mexicano del Carbono en colaboración con el Centro de Investigación Científica y de Educación Superior de Ensenada y la Universidad Autónoma de Baja California. Texcoco, pp. 272-277.

Delgadillo-Nuño, M.A., Liñán-Cabello, M.A., Delgadillo-Nuño, E., Galindo-Sánchez, C.E. & Carpizo-Ituarte, E. 2020. Gene expression plasticity in *Pocillopora* corals from 2 locations on the Carrizales Reef, Pacific coast of Mexico. Ciencias Marinas, 46: 89-100. doi: 10.7773/cm.v46i2.3062

DiMario, R.J., Machingura, M.C., Waldrop, G.L. & Moroney, J.V. 2018. The many types of carbonic anhydrases in photosynthetic organisms. Plant Science: An International Journal of Experimental Plant Biology, 268: 11-17. doi: 10.1016/j.plantsci. 2017.12.002

Dittami, S.M., Michel, G., Collén, J., Boyen, C. & Tonon, T. 2010. Chlorophyll-binding proteins revisited - A multigenic family of light-harvesting and stress proteins from a brown algal perspective. BMC Evolutionary Biology, 10: 1-14. doi: 10.1186/1471-2148-10-365

Donovan, M.K., Burkepile, D.E., Kratochwill, C., Schlesinger, T., Sully, S., Oliver, T.A., et al. 2021. Local conditions magnify coral loss after marine heatwaves. Science, 372: 977-980. doi: 10.1126/science. abd9464

Dove, S.G., Hoegh-Guldberg, O. & Ranganathan, S. 2001. Major colour patterns of reef-building corals are due to a family of GFP-like proteins. Coral Reefs, 19: 197-204. doi: 10.1007/PL00006956

Erez, J., Reynaud, S., Silverman, J., Schneider, K. & Allemand, D. 2011. Coral calcification under ocean acidification and global change. In: Dubinski, Z. & Stambler, N. (Eds.). Coral reefs: an ecosystem in transition. Springer Amsterdam, pp. 151-176.

Ferse, S.C.A., Hein, M.Y. & Rölfer, L. 2021. A survey of current trends and suggested future directions in coral transplantation for reef restoration. Plos One, 16: e0249966. doi: 10.1371/journal.pone.0249966

Fuess, L.E., Pinzón, C.J.H., Weil, E. & Mydlarz, L.D. 2016. Associations between transcriptional changes and protein phenotypes provide insights into immune regulation in corals. Developmental and Comparative Immunology, 62: 17-28. doi: 10.1016/j.dci.2016. 04.017

Gélin, P., Postaire, B., Fauvelot, C. & Magalon, H. 2017. Reevaluating species number, distribution and endemism of the coral genus *Pocillopora* Lamarck, 1816 using species delimitation methods and micro-satellites. Molecular Phylogenetics and Evolution, 109: 430-446. doi: 10.1016/ j.ympev.2017.01.018

González-Pech, R.A., Vargas, S., Francis, W.R. & Wörheide, G. 2017. Transcriptomic resilience of the *Montipora digitata* holobiont to low pH. Frontiers in Marine Science, 4: 403. doi: 10.3389/fmars.2017. 00403

Grabherr, M.G., Haas, B.J., Yassour, M., Levin, J.Z., Thompson, D.A., Amit, I., et al. 2011. Full-length transcriptome assembly from RNA-Seq data without a reference genome. Nature Biotechnology, 29: 644-652. doi: 10.1038/nbt.1883

Guo, Z., Liao, X., Han, T., Chen, J., He, C. & Lu, Z. 2021. Full-length transcriptomics reveals the gene expression profiles of reef-building coral *Pocillopora damicornis* and symbiont zooxanthellae. Diversity, 13: 543. doi: 10.3390/d13110543

Gutner-Hoch, E., Ben-Asher, H.W., Yam, R., Shemesh, A. & Levy, O. 2017. Identifying genes and regulatory pathways associated with the scleractinian coral calcification process. PeerJ, 2017: 3590. doi: 10.7717/ peerj.3590

Helmkampf, M., Bellinger, M.R., Frazier, M. & Takabayashi, M. 2019. Symbiont type and environmental factors affect transcriptome-wide gene expression in the coral *Montipora capitata*. Ecology and Evolution, 9: 378-392. doi: 10.1002/ece3.4756

Hernández-López, J., Cervantes, O., Olivos-Ortiz, A. & Guzmán-Reyna, R.R. 2020. DSPIR framework as planning and management tools for the La Boquita Coastal System, Manzanillo, Mexico. Journal of Marine Science and Engineering, 8: 615. doi: 10.3390/jmse8080615

Honaas, L.A., Altman, N.S. & Krzywinski, M. 2016. Study design for sequencing studies. In: Clifton, N.J. (Ed.). Methods in molecular biology. Humana Press, New York, pp. 39-66.

Hou, J., Xu, T., Su, D., Wu, Y., Cheng, L., Wang, J., et al. 2018. RNA-seq reveals extensive transcriptional response to heat stress in the stony coral *Galaxea fascicularis*. Frontiers in Genetics, 9: 37. doi: 10.3389/fgene.2018.00037

Huang, D.W., Sherman, B.T. & Lempicki, R.A. 2009. Systematic and integrative analysis of large gene lists using DAVID bioinformatics resources. Nature Protocols, 4: 44-57. doi: 10.1038/nprot.2008.211

Hwang, Y., Jung, G. & Jin, E.S. 2008. Transcriptome analysis of acclimatory responses to thermal stress in Antarctic algae. Biochemical and Biophysical Research Communications, 367: 635-641. doi: 10.1016/ j.bbrc.2007.12.176

Ishibashi, H., Takaichi, D. & Takeuchi, I. 2021. Effects of the herbicide Irgarol 1051 on the transcriptome of

hermatypic coral *Acropora tenuis* and its symbiotic dinoflagellates. Science of the Total Environment, 780: 146542. doi: 10.1016/j.scitotenv.2021.146542

Ishihara, T., Ifuku, K., Yamashita, E., Fukunaga, Y., Nishino, Y., Miyazawa, A., et al. 2015. Utilization of light by fucoxanthin-chlorophyll-binding protein in a marine centric diatom, *Chaetoceros gracilis*. Photosynthesis Research, 126: 437-447. doi: 10.1007/s11120-015-0170-5

Islas-Peña, T.V., Liñán-Cabello, M.A. & Torres-Orozco, E. 2013. Evaluation of two techniques for restoration of *Pocillopora* spp.: Early effects of species and marine environment. In: Corals: classification, habitat and ecological significance. Nova Science Publishers, New York, pp. 133-152.

Jatkar, A.A., Brown, B.E., Bythell, J.C., Guppy, R., Morris, N.J. & Pearson, J.P. 2010. Coral mucus: the properties of its constituent mucins. Biomacromolecules, 11: 883-888. doi: 10.1021/bm9012106

Johnston, E.C., Wyatt, A.S.J., Leichter, J.J. & Burgess, S.C. 2022. Niche differences in co-occurring cryptic coral species (*Pocillopora* spp.). Coral Reefs, 41: 767-778. doi: 10.1007/s00338-021-02107-9

Johnston, E.C., Forsman, Z.H., Flot, J.F., Schmidt-Roach, S., Pinzón, J.H., Knapp, I.S.S., et al. 2017. A genomic glance through the fog of plasticity and diversification in *Pocillopora*. Scientific Reports, 7: 1-11. doi: 10.1038/s41598-017-06085-3

Jusufi, J., Suormala, T., Burda, P., Fowler, B., Froese, D.S. & Baumgartner, M.R. 2014. Characterization of functional domains of the cblD (MMADHC) gene product. Journal of Inherited Metabolic Disease, 37: 841-849. doi: 10.1007/s10545-014-9709-4

Kirk, N.L., Howells, E.J., Abrego, D., Burt, J.A. & Meyer, E. 2018. Genomic and transcriptomic signals of thermal tolerance in heat-tolerant corals (*Platygyra daedalea*) of the Arabian/Persian Gulf. Molecular Ecology, 27: 5180-5194. doi: 10.1111/mec.14934

Koulen, P., Duncan, R.S., Liu, J., Cohen, N.E., Yannazzo, J.A.S., McClung, N., et al. 2005. Polycystin-2 accelerates Ca^{2+} release from intracellular stores in *Caenorhabditis elegans*. Cell Calcium, 37: 593-601. doi: 10.1016/j.ceca.2005.03.003

LaJeunesse, T.C., Parkinson, J.E., Gabrielson, P.W., Jeong, H.J., Reimer, J.D., Voolstra, C.R., et al. 2018. Systematic revision of Symbiodiniaceae highlights the antiquity and diversity of coral endosymbionts. Current Biology, 28: 2570-2580. doi: 10.1016/j.cub.2018.07.008

Langfelder, P. & Horvath, S. 2008. WGCNA: an R package for weighted correlation network analysis. BMC Bioinformatics, 9: 1-13. doi: 10.1186/1471-2105-9-559

Langmead, B. & Salzberg, S.L. 2012. Fast gapped-read alignment with Bowtie 2. Nature Methods, 9: 357-359. doi: 10.1038/nmeth.1923

Laurel-Sandoval, M.A.M. 2014. Caracterización de la comunidad bacteriana del coral *Pocillopora capitata* de los parches coralinos de Manzanillo, Colima. Centro de Investigación en Alimentación y Desarrollo, A.C., Mazatlán.

Li, B. & Dewey, C.N. 2011. RSEM: accurate transcript quantification from RNA-Seq data with or without a reference genome. BMC Bioinformatics, 12: 323. doi: 10.1186/1471-2105-12-323

Li, J., Long, L., Zou, Y. & Zhang, S. 2021. Microbial community and transcriptional responses to increased temperatures in coral *Pocillopora damicornis* holobiont. Environmental Microbiology, 23: 826-843. doi: 10.1111/1462-2920.15168

Libro, S., Kaluziak, S.T. & Vollmer, S.V. 2013. RNA-seq profiles of immune related genes in the staghorn coral *Acropora cervicornis* infected with white band disease. Plos One, 8: e81821. doi: 10.1371/journal.pone.0081821

Lin, S., Cheng, S., Song, B., Zhong, X., Lin, X., Li, W., et al. 2015. The *Symbiodinium kawagutii* genome illuminates dinoflagellate gene expression and coral symbiosis. Science, 350: 691-694. doi: 10.1126/science.aad0408

Liñán-Cabello, M.A. & Michel-Morfin, J.E. 2018. Recreational beaches as factors of involvement in a coral community: Colima case study. In: Botero, C.M., Cervantes, O. & Finkl, C.W. (Eds.). Beach management tools-concepts, methodologies, and case studies. Springer, Berlin, pp. 145-157.

Liñán-Cabello, M.A., Hernández-Medina, D., Florián-Álvarez, P. & Mena-Herrera, A. 2008. Estado actual del arrecife coralino "La Boquita," Colima. Iridia, 5: 10-23.

Liñán-Cabello, M.A., Flores-Ramírez, L.A., Laurel-Sandoval, M.A., Mendoza, E.G., Santiago, O.S. & Delgadillo-Nuño, M.A. 2011. Acclimation in *Pocillopora* spp. during a coral restoration program in Carrizales Bay, Colima, Mexico. Marine and Freshwater Behaviour and Physiology, 44: 61-72. doi: 10.1080/10236244.2010.537440

Liñán-Cabello, M.A., Olivos-Ortiz, A., Quijano-Scheggia, S., Anguiano, D.M., Reséndiz-Flores, M.L. & Ortega-Ortiz, C.D. 2016. Effects of terrestrial runoff on the coral communities in Santiago Bay, Colima, Mexican Pacific Coast. Revista de Biología Tropical, 64: 1185-1200. doi: 10.15517/rbt.v64i3.21817

Liu, Y., Jing, S.X., Luo, S.H. & Li, S.H. 2019. Non-volatile natural products in plant glandular trichomes:

chemistry, biological activities and biosynthesis. Natural Product Reports, 36: 626-665.

Liu, Y., Liao, X., Han, T., Su, A., Guo, Z., Lu, N., et al. 2021. Full-length transcriptome sequencing of the scleractinian coral *Montipora foliosa* reveals the gene expression profile of coral-Zooxanthellae holobiont. Biology, 10: 1274. doi: 10.3390/biology10121274

Lock, C., Bentlage, B. & Raymundo, L.J. 2022. Calcium homeostasis disruption initiates rapid growth after micro-fragmentation in the scleractinian coral *Porites lobata*. Ecology and Evolution, 12: 1-16. doi: 10.1002/ece3.9345

Love, M.I., Huber, W. & Anders, S. 2014. Moderated estimation of fold change and dispersion for RNA-seq data with DESeq2. Genome Biology, 15: 1-21. doi: 10.1186/s13059-014-0550-8

Maor-Landaw, K., Karako-Lampert, S., Ben-Asher, H.W., Goffredo, S., Falini, G., Dubinsky, Z., et al. 2014. Gene expression profiles during short-term heat stress in the red sea coral *Stylophora pistillata*. Global Change Biology, 20: 3026-3035. doi: 10.1111/gcb.12592

Mayfield, A.B., Wang, Y.B., Chen, C.S., Lin, C.Y. & Chen, S.H. 2014. Compartment-specific transcriptomics in a reef-building coral exposed to elevated temperatures. Molecular Ecology, 23: 5816-5830. doi: 10.1111/mec.12982

Mohamed, A.R., Cumbo, V., Harii, S., Shinzato, C., Chan, C.X., Ragan, M.A., et al. 2016. The transcriptomic response of the coral *Acropora digitifera* to a competent *Symbiodinium* strain: the symbiosome as an arrested early phagosome. Molecular Ecology, 25: 3127-3141. doi: 10.1111/mec.13659

Moya, A., Huisman, L., Ball, E.E., Hayward, D.C., Grasso, L.C., Chua, C.M., et al. 2012. Whole transcriptome analysis of the coral *Acropora millepora* reveals complex responses to CO_2-driven acidification during the initiation of calcification. Molecular Ecology, 21: 2440-2454. doi: 10.1111/j.1365-294X.2012.05554.x

Muñiz-Anguiano, D., Verduzco-Zapata, M. & Liñán-Cabello, M.A. 2017. Factores asociados a la respuesta de *Pocillopora* spp. (Anthozoa: Scleractinia) durante un proceso de restauración en la costa del Pacífico mexicano. Revista de Biología Marina y Oceanografía, 52: 299-310. doi: 10.4067/S0718-19572017000200009

Ng, C.S.L., Lim, J.X., Sam, S.Q., Kikuzawa, Y.P., Toh, T.C., Wee, T.W., et al. 2019. Variability in skeletal bulk densities of common hard corals in Southeast Asia. Coral Reefs, 38: 1133-1143. doi: 10.1007/s00338-019-01852-2

Nishiyama, Y., Allakhverdiev, S.I. & Murata, N. 2006. A new paradigm for the action of reactive oxygen species in the photoinhibition of photosystem II. Biochimica et Biophysica Acta, 1757: 742-749. doi: 10.1016/j.bbabio.2006.05.013

Nozawa, A., Nanamiya, H., Miyata, T., Linka, N., Endo, Y., Weber, A.P.M., et al. 2007. A cell-free translation and proteoliposome reconstitution system for functional analysis of plant solute transporters. Plant & Cell Physiology, 48: 1815-1820. doi: 10.1093/pcp/pcm150

Nymark, M., Valle, K.C., Brembu, T., Hancke, K., Winge, P., Andresen, K., et al. 2009. An integrated analysis of molecular acclimation to high light in the marine diatom *Phaeodactylum tricornutum*. Plos One, 4: e7743. doi: 10.1371/journal.pone.0007743

Olayioye, M.A., Vehring, S., Müller, P., Herrmann, A., Schiller, J., Thiele, C., et al. 2005. StarD10, a START domain protein overexpressed in breast cancer, functions as a phospholipid transfer protein. Journal of Biological Chemistry, 280: 27436-27442. doi: 10.1074/jbc.M413330200

Onyango, C.A., Glassom, D. & MacDonald, A. 2021. *De novo* assembly of the transcriptome of scleractinian coral, *Anomastraea irregularis* and analyses of its response to thermal stress. Molecular Biology Reports, 48: 2083-2092. doi: 10.1007/s11033-021-06184-5

Ostria-Hernández, M.L., Hernández-Zulueta, J., Vargas-Ponce, O., Díaz-Pérez, L., Araya, R., Rodríguez-Troncoso, A.P., et al. 2022. Core microbiome of corals *Pocillopora damicornis* and *Pocillopora verrucosa* in the northeastern tropical Pacific. Marine Ecology, 43: e12729. doi: 10.1111/maec.12729

Palmer, C.V. & Traylor-Knowles, N. 2012. Towards an integrated network of coral immune mechanisms. Proceedings of the Royal Society B: Biological Sciences, 279: 4106-4114. doi: 10.1098/RSPB.2012.1477

Palmer, C.V., Modi, C.K. & Mydlarz, L.D. 2009. Coral fluorescent proteins as antioxidants. Plos One, 4: e7298. doi: 10.1371/journal.pone.0007298

Park, S., Jung, G., Hwang, Y. & Jin, E.S. 2010. Dynamic response of the transcriptome of a psychrophilic diatom, *Chaetoceros neogracile*, to high irradiance. Planta, 231: 349-360. doi: 10.1007/s00425-009-1044-x

Patterson, K.L., Porter, J.W., Ritchie, K.B., Polson, S.W., Mueller, E., Peters, E.C., et al. 2002. The etiology of white pox, a lethal disease of the Caribbean elkhorn coral, *Acropora palmata*. Proceedings of the National Academy of Sciences of the United States of America, 99: 8725-8730. doi: 10.1073/pnas.092260099

Paz-García, D.A., Aldana-Moreno, A., Cabral-Tena, R.A., García-De-León, F.J., Hellberg, M.E. & Balart, E.F. 2015. Morphological variation and different branch modularity across contrasting flow conditions in dominant *Pocillopora* reef-building corals. Oecologia, 178: 207-218. doi: 10.1007/s00442-014-3199-9

Pinzón, J.H. & Lajeunesse, T.C. 2011. Species delimitation of common reef corals in the genus *Pocillopora* using nucleotide sequence phylogenies, population genetics and symbiosis ecology. Molecular Ecology, 20: 311-325. doi: 10.1111/j.1365-294X.2010.04939.x

Pinzón, J.H., Kamel, B., Burge, C.A., Harvell, C.D., Medina, M., Weil, E., et al. 2015. Whole transcriptome analysis reveals changes in expression of immune-related genes during and after bleaching in a reef-building coral. Royal Society Open Science, 2: 140214. doi: 10.1098/rsos.140214

Pinzón, J.H., Sampayo, E., Cox, E., Chauka, L.J., Chen, C.A., Voolstra, C.R., et al. 2013. Blind to morphology: genetics identifies several widespread ecologically common species and few endemics among Indo-Pacific cauliflower corals (*Pocillopora*, Scleractinia). Journal of Biogeography, 40: 1595-1608. doi: 10.1111/jbi.12110

Planes, S., Allemand, D., Agostini, S., Banaigs, B., Boissin, E., Boss, E., et al. 2019. The Tara Pacific expedition-A pan-ecosystemic approach of the "-omics" complexity of coral reef holobionts across the Pacific Ocean. Plos Biology, 17: e3000483. doi: 10.1371/journal.pbio.3000483

Poquita-Du, R.C., Goh, Y.L., Huang, D., Chou, L.M. & Todd, P.A. 2020. Gene expression and photophysiological changes in *Pocillopora acuta* coral holobiont following heat stress and recovery. Microorganisms, 8: 1-17. doi: 10.3390/microorganisms8081227

Poquita-Du, R.C., Huang, D., Chou, L.M. & Todd, P.A. 2019. Short term exposure to heat and sediment triggers changes in coral gene expression and photophysiological performance. Frontiers in Marine Science, 6: 121. doi: 10.3389/fmars.2019.00121

Quistad, S.D., Stotland, A., Barott, K.L., Smurthwaite, C.A., Hilton, B.J., Grasis, J.A., et al. 2014. Evolution of TNF-induced apoptosis reveals 550 My of functional conservation. Proceedings of the National Academy of Sciences of the United States of America, 111: 9567-9572. doi: 10.1073/pnas.1405912111

Reyes-Bermudez, A., Lin, Z., Hayward, D.C., Miller, D.J. & Ball, E.E. 2009. Differential expression of three galaxin-related genes during settlement and metamorphosis in the scleractinian coral *Acropora millepora*. BMC Evolutionary Biology, 9: 1-12. doi: 10.1186/1471-2148-9-178

Roder, C., Arif, C., Bayer, T., Aranda, M., Daniels, C., Shibl, A., et al. 2014. Bacterial profiling of white plague disease in a comparative coral species framework. The ISME Journal, 8: 31-39. doi: 10.1038/ismej.2013.127

Ross, C.L., Warnes, A., Comeau, S., Cornwall, C.E., Cuttler, M.V.W., Naugle, M., et al. 2022. Coral calcification mechanisms in a warming ocean and the interactive effects of temperature and light. Communications Earth & Environment, 3: 1-11. doi: 10.1038/s43247-022-00396-8

Ryu, T., Cho, W., Yum, S. & Woo, S. 2019. Holobiont transcriptome of colonial scleractinian coral *Alveopora japonica*. Marine Genomics, 43: 68-71. doi: 10.1016/j.margen.2018.07.003

Salih, A., Larkum, A., Cox, G., Kühl, M. & Hoegh-Guldberg, O. 2000. Fluorescent pigments in corals are photoprotective. Nature, 408: 850-853. doi: 10.1038/35048564

Sampayo, E.M., Ridgway, T., Franceschinis, L., Roff, G., Hoegh-Guldberg, O. & Dove, S. 2016. Coral symbioses under prolonged environmental change: living near tolerance range limits. Scientific Reports, 6: 36271. doi: 10.1038/srep36271

Savary, R., Barshis, D.J., Voolstra, C.R., Cárdenas, A., Evensen, N.R., Banc-Prandi, G., et al. 2021. Fast and pervasive transcriptomic resilience and acclimation of extremely heat-tolerant coral holobionts from the northern Red Sea. Proceedings of the National Academy of Sciences, 118: e2023298118. doi: 10.1073/pnas.2023298118

Schmidt-Roach, S., Miller, K.J., Lundgren, P. & Andreakis, N. 2014. With eyes wide open: a revision of species within and closely related to the *Pocillopora damicornis* species complex (Scleractinia; Pocilloporidae) using morphology and genetics. Zoological Journal of the Linnean Society, 170: 1-33. doi: 10.1111/zoj12092

Seneca, F.O. & Palumbi, S.R. 2015. The role of transcriptome resilience in resistance of corals to bleaching. Molecular Ecology, 24: 1467-1484. doi: 10.1111/mec.13125

Shinzato, C., Inoue, M. & Kusakabe, M. 2014a. A snapshot of a coral "holobiont": a transcriptome assembly of the scleractinian coral, *Porites*, captures a wide variety of genes from both the host and symbiotic zooxanthellae. Plos One, 9: e85182. doi: 10.1371/journal.pone.0085182

Shinzato, C., Mungpakdee, S., Satoh, N. & Shoguchi, E. 2014b. A genomic approach to coral-dinoflagellate symbiosis: studies of *Acropora digitifera* and *Symbiodinium minutum*. Frontiers in Microbiology, 5: 336. doi: 10.3389/fmicb.2014.00336

Shinzato, C., Khalturin, K., Inoue, J., Zayasu, Y., Kanda, M., Kawamitsu, M., et al. 2021. Eighteen coral genomes reveal the evolutionary origin of *Acropora* strategies to accommodate environmental changes. Molecular Biology and Evolution, 38: 16-30. doi: 10.1093/molbev/msaa216

Shinzato, C., Shoguchi, E., Kawashima, T., Hamada, M., Hisata, K., Tanaka, M., et al. 2011. Using the *Acropora digitifera* genome to understand coral responses to environmental change. Nature, 476: 320-323. doi: 10.1038/nature10249

Siebeck, U.E., Logan, D. & Marshall, N.J. 2008. CoralWatch - a flexible coral bleaching monitoring tool for you and your group. Proceedings of the 11th International Coral Reef Symposium, Nova Southeastern University, Florida.

Simão, F.A., Waterhouse, R.M., Ioannidis, P., Kriventseva, E.V. & Zdobnov, E.M. 2015. BUSCO: assessing genome assembly and annotation completeness with single-copy orthologs. Bioinformatics, 31: 3210-3212. doi: 10.1093/bioinformatics/btv351

Siu, K.K.W., Asmus, K., Zhang, A.N., Horvatin, C., Li, S., Liu, T., et al. 2011. Mechanism of substrate specificity in 5'-methylthioadenosine/S-adenosylhomocysteine nucleosidases. Journal of Structural Biology, 173: 86-98. doi: 10.1016/j.jsb.2010.06.006

Siu, K.K.W., Lee, J.E., Sufrin, J.R., Moffatt, B.A., McMillan, M., Cornell, K.A., et al. 2008. Molecular determinants of substrate specificity in plant 5'-methylthioadenosine nucleosidases. Journal of Molecular Biology, 378: 112-128. doi: 10.1016/j.jmb.2008.01.088

Smith, E.G., D'Angelo, C., Salih, A. & Wiedenmann, J. 2013. Screening by coral green fluorescent protein (GFP)-like chromoproteins supports a role in photoprotection of zooxanthellae. Coral Reefs, 32: 463-474. doi: 10.1007/s00338-012-0994-9

Smith-Unna, R., Boursnell, C., Patro, R., Hibberd, J.M. & Kelly, S. 2016. TransRate: reference-free quality assessment of de novo transcriptome assemblies. Genome Research, 26: 1134-1144. doi: 10.1101/gr.196469.115

Starcevic, A., Dunlap, W.C., Cullum, J., Malcolm, S.J., Hranueli, D. & Long, P.F. 2010. Gene expression in the scleractinian *Acropora microphthalma* exposed to high solar irradiance reveals elements of photoprotection and coral bleaching. Plos One, 5: e13975. doi: 10.1371/journal.pone.0013975

Strychar, K.B. & Sammarco, P.W. 2011. Effects of heat stress on phytopigments of Zooxanthellae (*Symbiodinium* spp.) symbiotic with the corals *Acropora hyacinthus*, *Porites solida*, and *Favites complanata*. International Journal of Biology, 4: 3-19. doi: 10.5539/ijb.v4n1p3

Studivan, M.S. & Voss, J.D. 2020. Transcriptomic plasticity of mesophotic corals among natural populations and transplants of *Montastraea cavernosa* in the Gulf of Mexico and Belize. Molecular Ecology, 29: 2399-2415. doi: 10.1111/mec.15495

Suggett, D.J. & Smith, D.J. 2020. Coral bleaching patterns are the outcome of complex biological and environmental networking. Global Change Biology, 26: 68-79. doi: 10.1111/gcb.14871

Sunagawa, S., DeSantis, T., Piceno, Y., Brodie, E.L., DeSalvo, M.K., Voolstra, C.R. et al. 2009. Bacterial diversity and white plague disease-associated community changes in the Caribbean coral *Montastraea faveolata*. The ISME Journal, 3: 512-521. doi: 10.1038/ismej.2008.131

Szklarczyk, D., Franceschini, A., Wyder, S., Forslund, K., Heller, D., Huerta-Cepas, J., et al. 2015. STRING v10: protein-protein interaction networks integrated over the tree of life. Nucleic Acids Research, 43: 447-452. doi: 10.1093/nar/gku1003

Szklarczyk, D., Morris, J.H., Cook, H., Kuhn, M., Wyder, S., Simonovic, M., et al. 2017. The STRING database in 2017: quality-controlled protein-protein association networks, made broadly accessible. Nucleic Acids Research, 45: 362-368. doi: 10.1093/nar/gkw937

Takagi, T., Yoshioka, Y., Zayasu, Y., Satoh, N. & Shinzato, C. 2020. Transcriptome analyses of immune system behaviors in primary polyp of coral *Acropora digitifera* exposed to the bacterial pathogen *Vibrio coralliilyticus* under thermal loading. Marine Biotechnology, 22: 748-759. doi: 10.1007/s10126-020-09984-1

Thomas, L., López, E.H., Morikawa, M.K. & Palumbi, S.R. 2019. Transcriptomic resilience, symbiont shuffling, and vulnerability to recurrent bleaching in reef-building corals. Molecular Ecology, 28: 3371-3382. doi: 10.1111/mec.15143

Thompson, J.R., Rivera, H.E., Closek, C.J. & Medina, M. 2015. Microbes in the coral holobiont: partners through evolution, development, and ecological interactions. Frontiers in Cellular and Infection Microbiology, 4: 176. doi: 10.3389/fcimb.2014.00176

Thurber, R.V., Willner-Hall, D., Rodriguez-Mueller, B., Desnues, C., Edwards, R.A., Angly, F., et al. 2009. Metagenomic analysis of stressed coral holobionts. Environmental Microbiology, 11: 2148-2163. doi: 10.1111/j.1462-2920.2009.01935.x

Toscanini, M.A., Favarolo, M.B., Gonzalez-Flecha, F.L., Ebert, B., Rautengarten, C. & Bredeston, L.M. 2019. Conserved Glu-47 and Lys-50 residues are critical for UDP-N-acetylglucosamine/UMP antiport activity of the mouse Golgi-associated transporter Slc35a3. Journal of Biological Chemistry, 294: 10042-10054. doi: 10.1074/jbc.RA119.008827

Tsuzuki, M. & Miyachi, S. 1989. The function of carbonic anhydrase in aquatic photosynthesis. Aquatic Botany, 34: 85-104. doi: 10.1016/0304-3770(89)90051-X

Ugrankar, R., Berglund, E., Akdemir, F., Tran, C., Kim, M.S., Noh, J., et al. 2015. *Drosophila* glucome screening identifies Ck1alpha as a regulator of mammalian glucose metabolism. Nature Communications, 6: 7102. doi: 10.1038/ncomms8102

Varasteh, T., Salazar, V., Tschoeke, D., Francini-Filho, R.B., Swings, J., Garcia, G., et al. 2021. *Breviolum* and *Cladocopium* are dominant among Symbiodiniaceae of the coral holobiont *Madracis decactis*. Microbial Ecology, 1: 1-11. doi: 10.1007/s00248-021-01868-8

Venn, A.A., Wilson, M.A., Trapido-Rosenthal, H.G., Keely, B.J. & Douglas, A.E. 2006. The impact of coral bleaching on the pigment profile of the symbiotic alga, *Symbiodinium*. Plant, Cell and Environment, 29: 2133-2142. doi: 10.1111/j.1365-3040.2006.001587.x

Vidal-Dupiol, J., Dheilly, N.M., Rondon, R., Grunau, C., Cosseau, C., Smith, K.M., et al. 2014. Thermal stress triggers broad *Pocillopora damicornis* transcriptomic remodeling, while *Vibrio coralliilyticus* infection induces a more targeted immuno-suppression response. Plos One, 9: e107672. doi: 10.1371/journal.pone.0107672

Vidal-Dupiol, J., Zoccola, D., Tambutté, E., Grunau, C., Cosseau, C., Smith, K.M., et al. 2013. Genes related to ion transport and energy production are upregulated in response to CO_2-driven pH decrease in corals: new insights from transcriptome analysis. Plos One, 8: e58652. doi: 10.1371/journal.pone.0058652

Wei, J., Kang, H.W. & Cohen, D.E. 2009. Thioesterase superfamily member 2 (Them2)/acyl-CoA thioesterase 13 (Acot13): a homotetrameric hotdog fold thioesterase with selectivity for long-chain fatty acyl-CoAs. Biochemical Journal, 421: 311-322. doi: 10.1042/BJ20090039

Williams, A.G., Thomas, S., Wyman, S.K. & Holloway, A.K. 2014. RNA-seq Data: challenges in and recommendations for experimental design and analysis. Current Protocols in Human Genetics, 83: 1-20. doi: 10.1002/0471142905.hg1113s83

Wright, R.M., Aglyamova, G.V., Meyer, E. & Matz, M.V. 2015. Gene expression associated with white syndromes in a reef building coral, *Acropora hyacinthus*. BMC Genomics, 16: 1-12. doi: 10.1186/s12864-015-1540-2

Yoshioka, Y., Yamashita, H., Suzuki, G. & Shinzato, C. 2022. Larval transcriptomic responses of a stony coral, *Acropora tenuis*, during initial contact with the native symbiont, *Symbiodinium microadriaticum*. Scientific Reports, 12: 1-11. doi: 10.1038/s41598-022-06822-3

Young, M.D., Wakefield, M.J., Smyth, G.K. & Oshlack, A. 2010. Gene ontology analysis for RNA-seq: accounting for selection bias. Genome Biology, 11: 1-12. doi: 10.1186/gb-2010-11-2-r14

Yuan, C., Zhou, Z., Zhang, Y., Chen, G., Yu, X., Ni, X., et al. 2017. Effects of elevated ammonium on the transcriptome of the stony coral *Pocillopora damicornis*. Marine Pollution Bulletin, 114: 46-52. doi: 10.1016/j.marpolbul.2016.08.036

Yuyama, I., Ishikawa, M., Nozawa, M., Yoshida, M. & Ikeo, K. 2018. Transcriptomic changes with increasing algal symbiont reveal the detailed process underlying establishment of coral-algal symbiosis. Scientific Reports, 8: 1-11. doi: 10.1038/s41598-018-34575-5

Zaccheo, O., Dinsdale, D., Meacock, P.A. & Glynn, P. 2004. Neuropathy target esterase and its yeast homologue degrade phosphatidylcholine to glycerophosphocholine in living cells. Journal of Biological Chemistry, 279: 24024-24033. doi: 10.1074/jbc.M400830200

Zhang, Y., Zhou, Z., Wang, L. & Huang, B. 2018. Transcriptome, expression, and activity analyses reveal a vital heat shock protein 70 in the stress response of stony coral *Pocillopora damicornis*. Cell Stress and Chaperones, 23: 711-721. doi: 10.1007/s12192-018-0883-4

Zhang, Y., Sun, J., Mu, H., Lun, J.C.Y. & Qiu, J.W. 2017. Molecular pathology of skeletal growth anomalies in the brain coral *Platygyra carnosa*: A meta-transcriptomic analysis. Marine Pollution Bulletin, 124: 660-667. doi: 10.1016/j.marpolbul.2017.03.047

Zhang, Y., Ip, J.C.H., Xie, J.Y., Yeung, Y.H., Sun, Y. & Qiu, J.W. 2022. Host-symbiont transcriptomic changes during natural bleaching and recovery in the leaf coral *Pavona decussata*. Science of the Total Environment, 806: 150656. doi: 10.1016/j.scitotenv.2021.150656

Zhou, Z., Zhang, G., Chen, G., Ni, X., Guo, L., Yu, X., et al. 2017. Elevated ammonium reduces the negative effect of heat stress on the stony coral *Pocillopora damicornis*. Marine Pollution Bulletin, 118: 319-327. doi: 10.1016/j.marpolbul.2017.03.018

Zhu, Y., Liao, X., Han, T., Chen, J.Y., He, C. & Lu, Z. 2022b. Symbiodiniaceae microRNAs and their targeting sites in coral holobionts: A transcriptomics-based exploration. Genomics, 114: 110404. doi: 10.1016/j.ygeno.2022.110404

Zhu, W., Zhu, M., Liu, X., Xia, J., Wang, H., Chen, R., et al. 2022a. Adaptive changes of coral *Galaxea fascicularis* holobiont in response to nearshore stress. Frontiers in Microbiology, 13: 1052776. doi: 10.3389/fmicb.2022.1052776

Received: October 17, 2022; Accepted: September 29, 2023

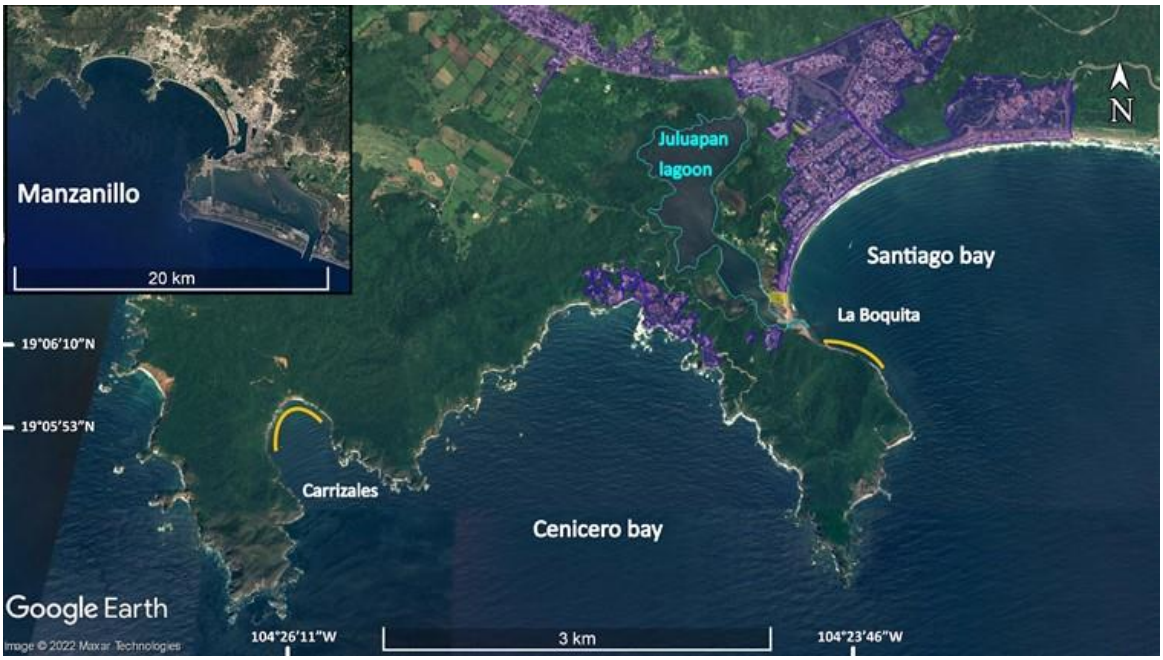

Figure S1. Map showing the locations of Carrizales and La Boquita reefs in Manzanillo, Colima, Mexico. The yellow lines show the location of the reefs where coral transplantations were performed. The urbanized area is shaded in purple. An artificial channel connects the Juluapan Lagoon with La Boquita Beach. This beach is a tourist site. Geographic coordinates of locations for coral's collection and transplantation are marked in the map (taken and modified from Google Earth 2022).

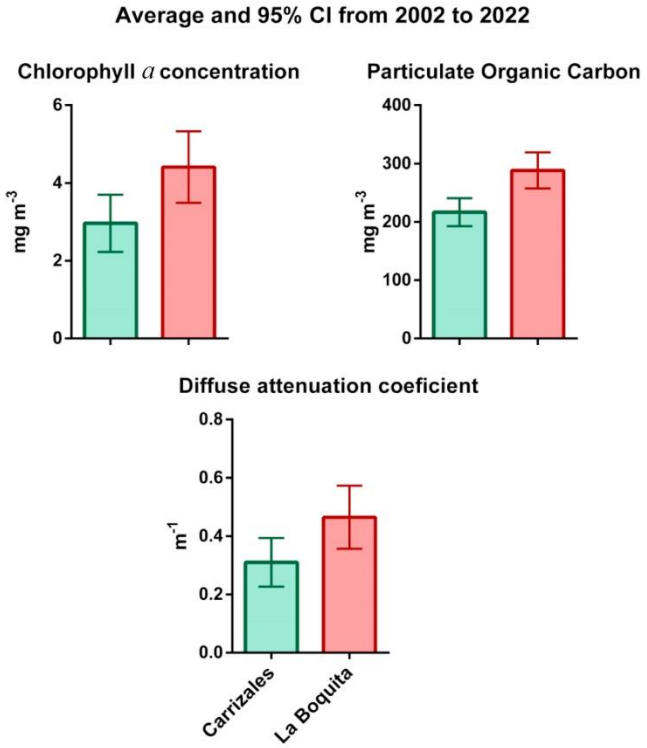

Figure S2. Area-averaged parameters (4 km^2) from the MODIS Aqua sensor (https://giovanni.gsfc.nasa.gov/), associated with water turbidity of both locations. Average and 95% confidence intervals (CI) of monthly satellite measurements from 2002 to 2022 are shown for each parameter. All the parameters were significantly higher ($P < 0.05$) at La Boquita, compared to Carrizales.

Figure S3. Left: *in situ* photograph of green and brown coral morphotypes of *Pocillopora grandis* cohabiting in Carrizales reef (Colima, Mexico); taken with a Sony camera (DSC-W350), exposure time 1/200 s, ISO 80; these colonies were not sampled. Right: *ex-situ* photograph of sampled fragments of both coral morphotypes used in the present study; taken under UV-light with a Nikon camera (D3300) with yellow UV filter, exposure time 1/2 s, ISO 3200.

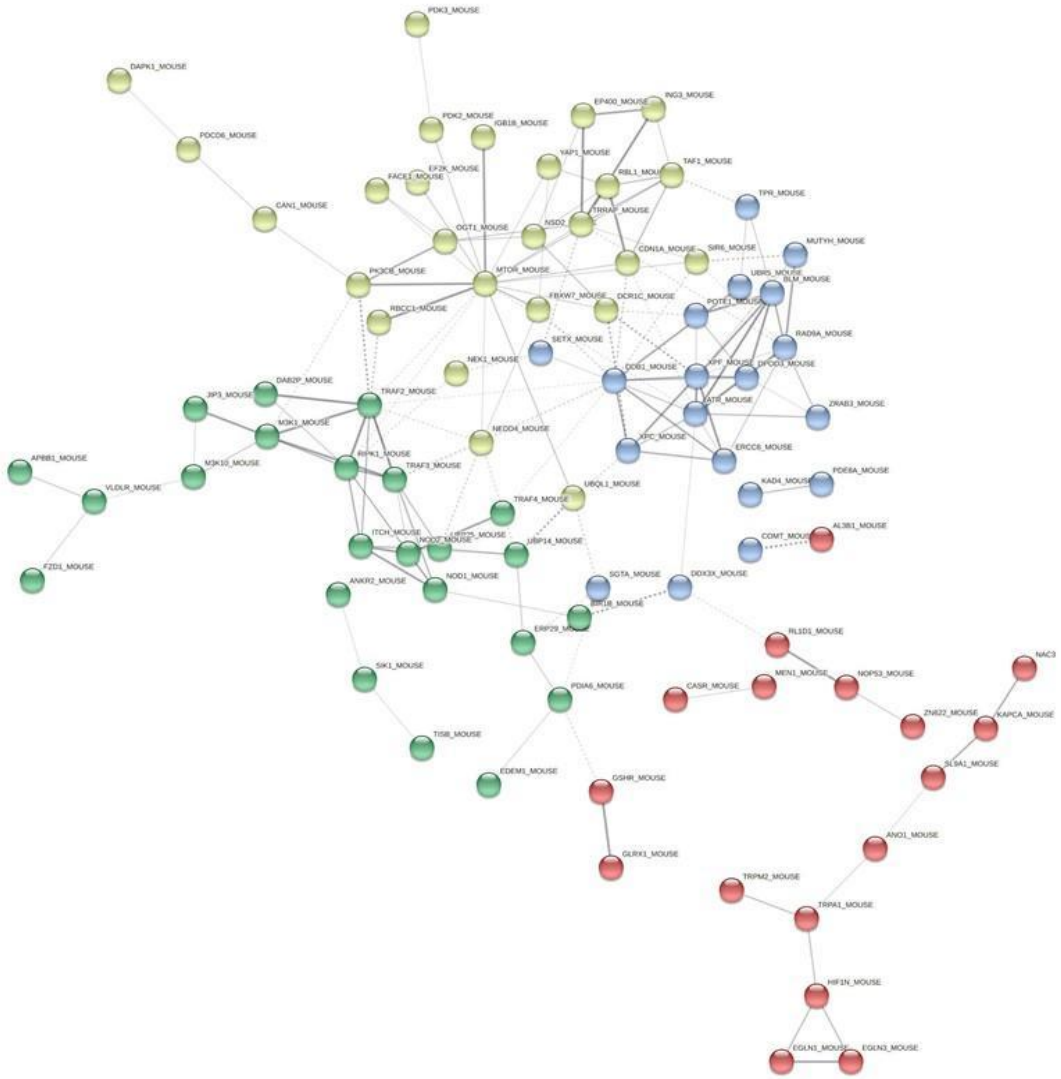

Figure S4. Animal-type protein interaction network associated with the stress response from the holobiont transcriptome of *Pocillopora grandis*. Interactions based on the mouse model. Colors represent interaction clusters based on confidence values.

Proteins in this network:

Node	Protein names
NSD2_MOUSE	[histone h3]-lysine36 n-dimethyltransferase nsd2
PDK2_MOUSE	[Pyruvate dehydrogenase (acetyl-transferring)] kinase isozyme 2, mitochondrial
PDK3_MOUSE	[Pyruvate dehydrogenase (acetyl-transferring)] kinase isozyme 3, mitochondrial
MUTYH_MOUSE	Adenine DNA glycosylase
KAD4_MOUSE	Adenylate kinase 4, mitochondrial
AL3B1_MOUSE	Aldehyde dehydrogenase family 3 member B1
APBB1_MOUSE	Amyloid beta (a4) precursor protein-binding, family b, member 1
ANKL1_MOUSE	Ankyrin repeat and LEM domain-containing protein 1
ANKR2_MOUSE	Ankyrin repeat domain 2 (stretch responsive muscle)
ANO1_MOUSE	Anoctamin-1
LOX5_MOUSE	Arachidonate 5-lipoxygenase
ATR_MOUSE	Ataxia telangiectasia and rad3 related
ABCA7_MOUSE	ATP-binding cassette sub-family A member 7
DDX3X_MOUSE	ATP-dependent RNA helicase DDX3X
DUS19_MOUSE	Atypical dual specificity phosphatase
BIR1B_MOUSE	Baculoviral IAP repeat-containing protein 1b
BLM_MOUSE	Bloom syndrome protein homolog
FACE1_MOUSE	CAAX prenyl protease 1 homolog
CAN1_MOUSE	Calpain-1 catalytic subunit
KAPCA_MOUSE	cAMP-dependent protein kinase catalytic subunit alpha
COMT_MOUSE	Catechol o-methyltransferase
RAD9A_MOUSE	Cell cycle checkpoint control protein RAD9A
JIP4_MOUSE	C-Jun-amino-terminal kinase-interacting protein 4
CDN1A_MOUSE	Cyclin-dependent kinase inhibitor 1
DAPK1_MOUSE	Death-associated protein kinase 1
DTX3L_MOUSE	Deltex 3-like, e3 ubiquitin ligase
DAB2P_MOUSE	Disabled homolog 2-interacting protein
DDR2_MOUSE	Discoidin domain receptor family member 2
ZRAB3_MOUSE	DNA annealing helicase and endonuclease ZRANB3
DCR1C_MOUSE	DNA cross-link repair 1c protein
DDB1_MOUSE	DNA damage-binding protein 1
XPC_MOUSE	DNA repair protein complementing XP-C cells homolog
EP400_MOUSE	E1A-binding protein p400
ITCH_MOUSE	E3 ubiquitin-protein ligase Itchy
ERP29_MOUSE	Endoplasmic reticulum resident protein 29
EDEM1_MOUSE	ER degradation-enhancing alpha-mannosidase-like protein 1
EF2K_MOUSE	Eukaryotic elongation factor-2 kinase
XPF_MOUSE	Excision repair cross-complementing rodent repair deficiency, complementation group 4
ERCC6_MOUSE	Excision repair cross-complementing rodent repair deficiency, complementation group 6
CASR_MOUSE	Extracellular calcium-sensing receptor
FBXW7_MOUSE	F-box/WD repeat-containing protein 7
FZD1_MOUSE	Frizzled class receptor 1
FKTN_MOUSE	Fukutin
GPS2_MOUSE	G protein pathway suppressor 2
GLRX1_MOUSE	Glutaredoxin-1
GSHR_MOUSE	Glutathione reductase, mitochondrial
PDE8A_MOUSE	High affinity cAMP-specific and IBMX-insensitive 3',5'-cyclic phosphodiesterase 8A
HIF1N_MOUSE	Hypoxia-inducible factor 1-alpha inhibitor (HIF hydroxylase)
EGLN1_MOUSE	Hypoxia-inducible factor prolyl hydroxylase
EGLN3_MOUSE	Hypoxia-inducible factor prolyl hydroxylase
IGB1B_MOUSE	Immunoglobulin (cd79a) binding protein 1b
IMPCT_MOUSE	Impact, RWD domain protein

Continuation

Node	Protein names
ING3_MOUSE	Inhibitor of growth protein 3
LONM_MOUSE	Lon protease homolog, mitochondrial
MBOA5_MOUSE	Lysophospholipid acyltransferase 5
MARH7_MOUSE	Membrane-associated ring-ch-type finger 7
JIP3_MOUSE	Mitogen-activated protein kinase 8 interacting protein 3
M3K1_MOUSE	Mitogen-activated protein kinase kinase kinase 1
M3K10_MOUSE	Mitogen-activated protein kinase kinase kinase 10
TISB_MOUSE	mRNA decay activator protein ZFP36L1
MEN1_MOUSE	Multiple endocrine neoplasia 1
MYEF2_MOUSE	Myelin expression factor 2
SIR6_MOUSE	NAD-dependent protein deacetylase sirtuin-6
NEO1_MOUSE	Neogenin
NEDD4_MOUSE	Neural precursor cell expressed, developmentally down-regulated 4
NEK1_MOUSE	Nima (never in mitosis gene a)-related expressed kinase 1
NEK4_MOUSE	Nima (never in mitosis gene a)-related expressed kinase 4
NUAK1_MOUSE	NUAK family SNF1-like kinase 1
TPR_MOUSE	Nucleoprotein TPR
NOD1_MOUSE	Nucleotide-binding oligomerization domain-containing protein 1
NOD2_MOUSE	Nucleotide-binding oligomerization domain-containing protein 2
OGT1_MOUSE	O-linked N-acetylglucosamine (GlcNAc) transferase
PK3CB_MOUSE	Phosphatidylinositol-4,5-bisphosphate 3-kinase catalytic subunit alpha/beta/delta
PLS1_MOUSE	Phospholipid scramblase 1
DPOD3_MOUSE	Polymerase (DNA-directed), delta 3, accessory subunit
SETX_MOUSE	Probable helicase senataxin
PDCD6_MOUSE	Programmed cell death protein 6
POTE1_MOUSE	Protection of telomeres protein 1
PDIA6_MOUSE	Protein disulfide isomerase associated 6
XYLT1_MOUSE	Protein xylosyltransferase
YPEL3_MOUSE	Protein Yippee-like 3
PSA_MOUSE	Puromycin-sensitive aminopeptidase
RBCC1_MOUSE	RB1-inducible coiled-coil protein 1
RIPK1_MOUSE	Receptor-interacting serine/threonine-protein kinase 1
RBL1_MOUSE	Retinoblastoma-like protein 1
RL1D1_MOUSE	Ribosomal L1 domain-containing protein 1
NOP53_MOUSE	Ribosome biogenesis protein NOP53
MTOR_MOUSE	Serine/threonine-protein kinase mTOR
SIK1_MOUSE	Serine/threonine-protein kinase SIK1
SGTA_MOUSE	Small glutamine-rich tetratricopeptide repeat-containing protein alpha
NRAM2_MOUSE	Solute carrier family 11 (proton-coupled divalent metal ion transporters), member 2
SCMC1_MOUSE	Solute carrier family 25 (mitochondrial phosphate transporter), member 23/24/25/41
S38A3_MOUSE	Solute carrier family 38 (sodium-coupled neutral amino acid transporter), member 3
NAC3_MOUSE	Solute carrier family 8 (sodium/calcium exchanger), member 3
SL9A1_MOUSE	Solute carrier family 9 (sodium/hydrogen exchanger), member 1
SMHD1_MOUSE	Structural maintenance of chromosomes flexible hinge domain-containing protein 1
TBC24_MOUSE	TBC1 domain family member 24
TRAF2_MOUSE	TNF receptor-associated factor 2
TRAF3_MOUSE	TNF receptor-associated factor 3
TRAF4_MOUSE	TNF receptor-associated factor 4
TAF1_MOUSE	Transcription initiation factor TFIID subunit 1
YAP1_MOUSE	Transcriptional coactivator YAP1

Continuation

Node	Protein names
TRRAP_MOUSE	Transformation/transcription domain-associated protein
TRPA1_MOUSE	Transient receptor potential cation channel subfamily A member 1
TRPM2_MOUSE	Transient receptor potential cation channel subfamily M member 2
UBQL1_MOUSE	Ubiquilin-1
UBP14_MOUSE	Ubiquitin carboxyl-terminal hydrolase 14
UBP25_MOUSE	Ubiquitin carboxyl-terminal hydrolase 25
UBR5_MOUSE	Ubiquitin protein ligase e3 component n-recognin 5
VLDLR_MOUSE	Very low-density lipoprotein receptor
ZN622_MOUSE	Zinc finger protein 622

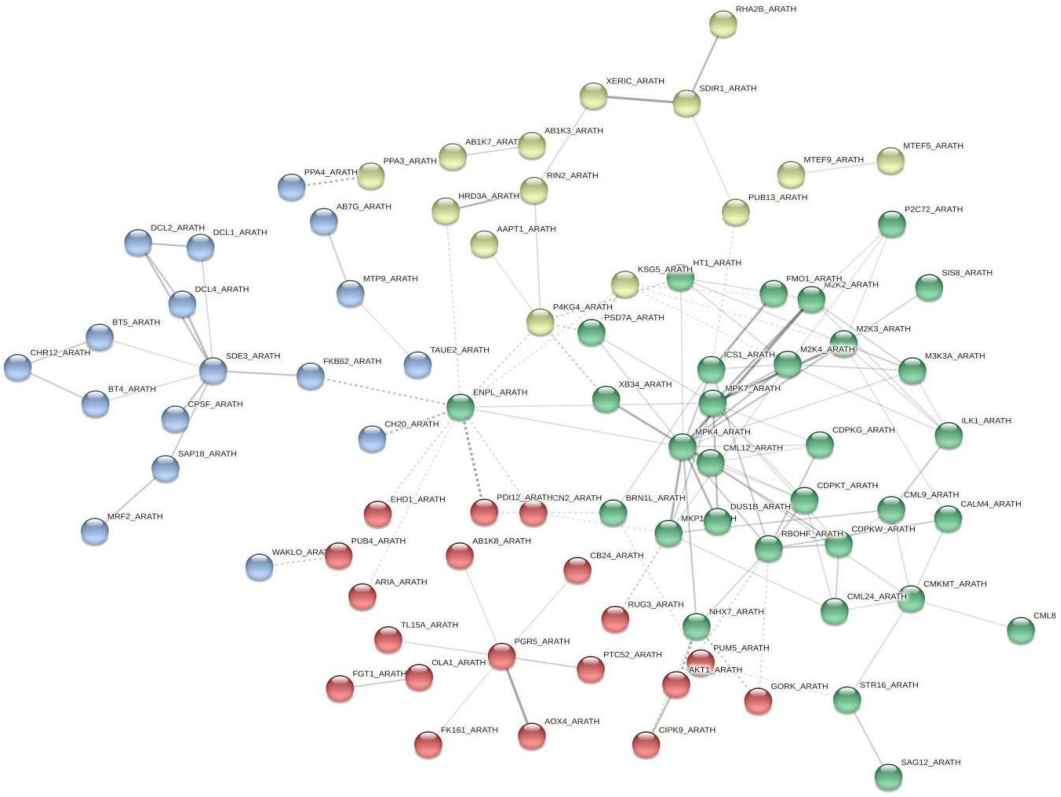

Figure S5. Plant-type protein interaction network associated with the stress response from the holobiont transcriptome of *Pocillopora grandis*. Interactions based on *Arabidopsis thaliana*. Colors represent interaction clusters based on confidence values.

Proteins in this network:

Node name	Protein names
PSD7A_ARATH	26S proteasome non-ATPase regulatory subunit 7 homolog A
AB7G_ARATH	ABC-2 type transporter family protein
FACR5_ARATH	Alcohol-forming fatty acyl-CoA reductase
TIL_ARATH	Apolipoprotein D and lipocalin family protein
CCL11_ARATH	Arginine-rich cyclin 1
ARIA_ARATH	ARM repeat protein interacting with ABF2
RIN2_ARATH	Autocrine motility factor receptor
LFG4_ARATH	Bax inhibitor-1 family protein
BPM2_ARATH	BTB/POZ and MATH domain-containing protein 2
BT4_ARATH	BTB/POZ and TAZ domain-containing protein 4
BT5_ARATH	BTB/POZ and TAZ domain-containing protein 5
Y1576_ARATH	BTB/POZ domain-containing protein At1g55760
CSE_ARATH	Caffeoyl shikimate esterase
PPA4_ARATH	Calcineurin-like metallo-phosphoesterase superfamily protein
CML8_ARATH	Calcium-binding protein cml
CML9_ARATH	Calcium-binding protein cml
CDPKG_ARATH	Calcium-dependent protein kinase 16
CDPKT_ARATH	Calcium-dependent protein kinase 29
CDPKW_ARATH	Calcium-dependent protein kinase 32
CALM4_ARATH	Calmodulin 1
CML12_ARATH	Calmodulin like 4
MTP9_ARATH	Cation efflux family protein
CIPK9_ARATH	CBL-interacting serine/threonine-protein kinase 9
ENPL_ARATH	Chaperone protein HtpG family protein
CH20_ARATH	Chloroplast chaperonin 10
AAPT1_ARATH	Choline/ethanolaminephosphotransferase 1
CPSF_ARATH	Cleavage and polyadenylation specificity factor 30
CRK13_ARATH	Cysteine-rich RLK (receptor-like protein kinase) 13
FMO1_ARATH	Dimethylaniline monooxygenase (n-oxide forming)
GRDP1_ARATH	DNA-binding protein, putative (duplicated duf1399)
DUS1B_ARATH	Dual specificity protein phosphatase 1B
RHA2B_ARATH	E3 ubiquitin-protein ligase RHA2B
RHC1A_ARATH	E3 ubiquitin-protein ligase RNF115/126
CML24_ARATH	EF hand calcium-binding protein family
EHD1_ARATH	EH domain-containing protein 1
HRD3A_ARATH	EMS-mutagenized bri1 suppressor 5
DCL4_ARATH	Endoribonuclease Dicer
DCL1_ARATH	Endoribonuclease Dicer homolog 1
DCL2_ARATH	Endoribonuclease Dicer homolog 2
ICS1_ARATH	Enhanced disease susceptibility to Erysiphe orontii 16
FK161_ARATH	FKBP-like peptidyl-prolyl cis-trans isomerase family protein
GORK_ARATH	Gated outwardly-rectifying K+ channel
GLAK2_ARATH	GHMP kinase family protein
GRXC2_ARATH	Glutaredoxin family protein
OLA1_ARATH	GTP binding protein
SAP18_ARATH	Histone deacetylase complex subunit SAP18
ILK1_ARATH	Integrin-linked protein kinase family
CEPR2_ARATH	Leucine-rich receptor-like protein kinase family protein
Y5639_ARATH	Leucine-rich repeat protein kinase family protein
CB24_ARATH	Light-harvesting complex II chlorophyll a/b binding protein 2
MRF2_ARATH	MA3 domain-containing protein
NFD4_ARATH	Major facilitator superfamily protein
MPI2_ARATH	Mannose-6-phosphate isomerase, type I
M3K3A_ARATH	MEK kinase (MAP3Ka)

Continuation

Node name	Protein names
MTEF5_ARATH	Mitochondrial transcription termination factor family protein
MTEF9_ARATH	Mitochondrial transcription termination factor family protein
MPK4_ARATH	Mitogen-activated protein kinase 4
MPK7_ARATH	Mitogen-activated protein kinase 7/14
M2K2_ARATH	Mitogen-activated protein kinase kinase 2
M2K3_ARATH	Mitogen-activated protein kinase kinase 3
M2K4_ARATH	Mitogen-activated protein kinase kinase 4
MKP1_ARATH	Mitogen-activated protein kinase phosphatase 1
NHD1_ARATH	NA/H antiporter 1
AKRC9_ARATH	NADPH-dependent aldo-keto reductase, chloroplastic
AB1K8_ARATH	Oxidative stress-related abc1-like protein 1
COAD_ARATH	Pantetheine-phosphate adenylyltransferase
PP213_ARATH	Pentatricopeptide repeat-containing protein At3g04760, chloroplastic
FKB62_ARATH	Peptidyl-prolyl cis-trans isomerase FKBP62
P4KG4_ARATH	Phosphatidylinositol 4-kinase gamma 4
SFH7_ARATH	Phosphatidylinositol/phosphatidylcholine transfer protein SFH7
PUB13_ARATH	Plant U-box 13
SDE3_ARATH	P-loop containing nucleoside triphosphate hydrolases superfamily protein
PARG1_ARATH	Poly (ADP-ribose) glycohydrolase (PARG)
AKT1_ARATH	Potassium channel AKT1
HMA1_ARATH	Probable cadmium/zinc-transporting ATPase HMA1, chloroplastic
Y3148_ARATH	Probable leucine-rich repeat receptor-like serine/threonine-protein kinase At3g14840
PDI12_ARATH	Protein disulfide isomerase-like 1-2
GCN2_ARATH	Protein kinase family protein
AB1K3_ARATH	Protein kinase superfamily protein
AB1K7_ARATH	Protein kinase superfamily protein
P2C72_ARATH	Protein phosphatase 2C family protein
PGR5_ARATH	Protein proton gradient regulation 5, chloroplastic
SIS8_ARATH	Protein tyrosine kinase family protein
PUM5_ARATH	Pumilio RNA-binding family
PPA18_ARATH	Purple acid phosphatase 18 (PAP18)
PPA3_ARATH	Purple acid phosphatase 3 (PAP3)
XB34_ARATH	Putative E3 ubiquitin-protein ligase XBAT34
PP239_ARATH	Putative pentatricopeptide repeat-containing protein at3g16890, mitochondrial
RUG3_ARATH	Regulator of chromosome condensation (RCC1) family protein
RBOHF_ARATH	Respiratory burst oxidase homolog protein F
FGT1_ARATH	RING/FYVE/PHD zinc finger superfamily protein
XERIC_ARATH	RING/U-box domain-containing protein
ATL8_ARATH	RING/U-box superfamily protein
PUB4_ARATH	RING/U-box superfamily protein with ARM repeat domain
BRN1L_ARATH	RNA-binding protein-defense related 1
CMKMT_ARATH	S-adenosyl-L-methionine-dependent methyltransferases superfamily protein
SDIR1_ARATH	Salt- and drought-induced RING finger1
SAG12_ARATH	Senescence-specific cysteine protease SAG12
SCP33_ARATH	Serine carboxypeptidase-like Clade II
HT1_ARATH	Serine/threonine-protein kinase HT1
KSG5_ARATH	Shaggy-related protein kinase epsilon
LSM1B_ARATH	Small nuclear ribonucleoprotein family protein
CHR12_ARATH	SNF2/Brahma-type chromatin-remodeling protein CHR12
NHX7_ARATH	Sodium proton exchanger, putative (NHX7) (SOS1)
BAC2_ARATH	Solute carrier family 25 (mitochondrial carnitine/acylcarnitine transporter), member 20/29
SRK2J_ARATH	Sucrose nonfermenting 1-related protein kinase 2-9
TAUE2_ARATH	Sulfite exporter TauE/SafE family protein

Continuation

Node name	Protein names
TL15A_ARATH	Tetratricopeptide repeat (TPR)-like superfamily protein
STR16_ARATH	Thiosulfate sulfurtransferase 16, chloroplastic
PTC52_ARATH	Translocon at the inner envelope membrane of chloroplasts, 55 KDA - IV
AVT1D_ARATH	Transmembrane amino acid transporter family protein
AOX4_ARATH	Ubiquinol oxidase 4, chloroplastic/chromoplastic
U76E2_ARATH	UDP-glucosyl transferase 76E2
VP53A_ARATH	Vacuolar protein sorting-associated protein 53
WAKLO_ARATH	Wall-associated receptor kinase-like 14
AB11G_ARATH	White-brown complex homolog protein 11

Table S1. BLAST hits against the GenBank database of sequences used for molecular identification of coral and endosymbiont species. *Pocillopora grandis* is the senior synonym of *Pocillopora eydouxi*; *Durusdinium* sp. was formerly classified as *Symbiodinium* clade *D.*

Coral identification	Scientific name	E-value	Ident. (%)
TRINITY_DN98458_c0_g1_i1: Cytochrome c oxidase subunit 1			
EF526303.1	*Pocillopora grandis*	0	100.0
KY887487.1	*Pocillopora grandis*	0	100.0
NC_009797.1	*Pocillopora damicornis*	0	99.49
EU400213.1	*Pocillopora damicornis*	0	99.36
TRINITY_DN68564_c0_g1_i1: rRNA large subunit			
EF526303.1	*Pocillopora grandis*	0	100.0
NC_009797.1	*Pocillopora damicornis*	0	99.91
EU400213.1	*Pocillopora damicornis*	0	99.73
NC_011162.1	*Stylophora pistillata*	0	98.49
TRINITY_DN3780_c0_g1_i1: rRNA small subunit			
EF526303.1	*Pocillopora grandis*	0	99.90
NC_009797.1	*Pocillopora damicornis*	0	99.81
EF596976.1	*Pocillopora meandrina*	0	99.72
AF333043.1	*Pocillopora damicornis*	0	99.72
Endosymbiont identification	**Scientific name**	**E-value**	**Ident. (%)**
TRINITY_DN38466_c0_g4_i1: Ribulose-1,5 bisphosphate carboxylase/oxygenase			
MN148731.1	*Durusdinium* sp.	0	96.07
JQ926157.1	*Symbiodinium* sp. clade B	0	90.05
JQ926156.1	*Symbiodinium* sp. clade B	0	90.04
JQ926158.1	*Symbiodinium* sp. clade B	0	89.69
TRINITY_DN39813_c1_g1_i1: Photosystem II protein D1			
JQ003851.1	*Durusdinium* sp. D1a	2.0E-75	96.61
AB086878.1	*Symbiodinium* sp. HPiH-2	5.0E-82	96.35
MH257967.1	*Symbiodinium* sp.	7.0E-66	94.19
MH257961.1	*Symbiodinium* sp.	7.0E-66	94.19
TRINITY_DN32493_c0_g1_i1: Photosystem I P700 chlorophyll a apoprotein A1			
JX624224.1	*Symbiodinium* sp. clade D4-5	0	96.61
JX624222.1	*Symbiodinium* sp. B1	2.0E-121	89.13
JX094317.1	*Symbiodinium* sp. Mf1.05b	0	86.76
JX094316.1	*Symbiodinium* sp. Mf1.05b	0	86.76

Table S2. Enrichment of GO terms for DEGs from pairwise comparisons between transplant locations (Carrizales *vs.* Boquita) and color morphotypes (green *vs.* brown) of *Pocillopora grandis* holobiont. GO: gene ontology; DEGs: differentially expressed genes.

Green Up	Term	*P*-value
GO:0019543	propionate catabolic process	9.79E-03
GO:0050427	3'-phosphoadenosine 5'-phosphosulfate metabolic process	1.99E-02
GO:0046327	glycerol biosynthetic process from pyruvate	2.25E-02
GO:1990764	myofibroblast contraction	2.37E-02
GO:0006122	mitochondrial electron transport, ubiquinol to cytochrome c	2.70E-02
GO:0048268	clathrin coat assembly	2.97E-02
GO:0070365	hepatocyte differentiation	3.33E-02
GO:0008218	bioluminescence	3.36E-02
Brown Up		
GO:0042694	muscle cell fate specification	6.00E-03
GO:2000773	negative regulation of cellular senescence	7.32E-03
GO:0035282	segmentation	9.55E-03
GO:0038027	apolipoprotein A-I-mediated signaling pathway	1.05E-02
GO:0060509	type I pneumocyte differentiation	1.05E-02
GO:2000427	positive regulation of apoptotic cell clearance	1.75E-02
GO:1903897	regulation of PERK-mediated unfolded protein response	2.10E-02
GO:0042985	negative regulation of amyloid precursor protein biosynthetic process	2.10E-02
Boquita Up		
GO:0009765	photosynthesis, light harvesting	1.83E-06
GO:0018298	protein-chromophore linkage	1.96E-05
GO:0020028	endocytic hemoglobin import into the cell	2.17E-05
GO:0071320	cellular response to cAMP	1.03E-04
GO:0032874	positive regulation of stress-activated MAPK cascade	1.87E-03
GO:0090135	actin filament branching	6.00E-03
GO:0030010	establishment of cell polarity	2.02E-02
GO:0015976	carbon utilization	3.87E-02
Carrizales Up		
GO:0019685	photosynthesis, dark reaction	8.46E-05
GO:0035990	tendon cell differentiation	6.00E-03
GO:0035914	skeletal muscle cell differentiation	1.06E-02
GO:0060153	modulation by virus of host cell cycle	1.10E-02
GO:0007535	donor selection	1.17E-02
GO:0060543	negative regulation of strand invasion	1.17E-02
GO:0042758	long-chain fatty acid catabolic process	1.29E-02
GO:0019265	glycine biosynthetic process, by transamination of glyoxylate	1.30E-02

Table S3. Top 50 DEGs of *Pocillopora grandis* holobionts transplanted at La Boquita reef *vs.* transplanted at Carrizales reef in Colima, Mexico. Normalized gene expression values are shown for each sample (counts per million). Positive $\log_2$ (fold change) values indicate upregulation in La Boquita, while negative values indicate upregulation in Carrizales. P. adj.: adjusted *P*-value after Benjamini-Hochberg procedure.

Transcript ID	BlastP	$\log_2$ (Fold Change)	P. adj.	Boquita brown	Boquita green	Carrizales brown	Carrizales green	Sample A	Sample B
lcl|TRINITY_DN42561_c0_g1_i1	Peroxidasin homolog PXN-2	3.66	3.24E-57	178,872	153,096	15,281	11,034	Boquita	Carrizales
lcl|TRINITY_DN41053_c0_g1_i5	Fucoxanthin-chlorophyll a-c binding protein F, chloroplastic	4.57	4.87E-30	37,062	40,027	1,287	1,922	Boquita	Carrizales
lcl|TRINITY_DN40414_c0_g1_i14	Fumarate reductase	2.94	3.77E-27	63,51	71,559	7,776	9,766	Boquita	Carrizales
lcl|TRINITY_DN42192_c0_g1_i1	Pyruvate:ferredoxin oxidoreductase	5.64	4.26E-15	8,153	9,002	0,178	0,176	Boquita	Carrizales
lcl|TRINITY_DN39574_c0_g1_i1	Serine/threonine-protein kinase SIK1	5.59	7.84E-13	104,959	42,183	1,371	1,707	Boquita	Carrizales
lcl|TRINITY_DN8170_c0_g1_i1	Protein MEI2-like 5	4.59	1.78E-11	10,634	11,333	0,262	0,644	Boquita	Carrizales
lcl|TRINITY_DN67632_c0_g1_i1	Isoamylase 3, chloroplastic	3.11	2.93E-11	9,519	9,041	0,806	1,356	Boquita	Carrizales
lcl|TRINITY_DN45708_c0_g1_i8	Heat shock protein 90	2.09	5.11E-11	224,709	274,455	45,916	71,093	Boquita	Carrizales
lcl|TRINITY_DN42817_c0_g1_i1	Fucoxanthin-chlorophyll a-c binding protein B, chloroplastic	3.4	1.06E-10	73,842	88,413	6,227	9,005	Boquita	Carrizales
lcl|TRINITY_DN56274_c0_g1_i1	Carotenoid-cleaving dioxygenase, mitochondrial	2.78	4.09E-10	13,686	17,185	1,716	2,781	Boquita	Carrizales
lcl|TRINITY_DN38766_c0_g1_i3	Carbonic anhydrase 2	2.35	1.03E-09	120,844	117,546	18,002	28,751	Boquita	Carrizales
lcl|TRINITY_DN41619_c1_g3_i1	Hexokinase HKDC1	4.01	6.35E-09	36,961	15,79	1,193	2,088	Boquita	Carrizales
lcl|TRINITY_DN57537_c0_g1_i1	ABC transporter G family member 24	3.77	2.29E-08	2,681	4,652	0,23	0,302	Boquita	Carrizales
lcl|TRINITY_DN39737_c1_g3_i2	Glyceraldehyde-3-phosphate dehydrogenase 2	2.85	3.04E-08	22,281	21,301	2,669	3,444	Boquita	Carrizales
lcl|TRINITY_DN38445_c0_g1_i1	Matrix metalloproteinase-19	3.67	3.61E-08	49,984	17,37	1,716	3,639	Boquita	Carrizales
lcl|TRINITY_DN98659_c0_g1_i1	Calcium-dependent protein kinase 2	3.88	7.65E-08	6,055	5,276	0,293	0,478	Boquita	Carrizales
lcl|TRINITY_DN90574_c0_g1_i1	Phosphatidylinositol 4-phosphate 5-kinase 4	3.17	8.44E-08	14,389	16,093	1,382	2	Boquita	Carrizales
lcl|TRINITY_DN39166_c0_g2_i1	Ribulose bisphosphate carboxylase, chloroplastic	3.52	9.13E-08	37,212	39,939	2,972	3,844	Boquita	Carrizales
lcl|TRINITY_DN40633_c4_g2_i1	Caroteno-chlorophyll a-c-binding protein	4.62	1.13E-07	26,468	28,587	0,848	1,385	Boquita	Carrizales
lcl|TRINITY_DN40879_c1_g3_i1	Eukaryotic translation initiation factor 3 subunit A	5.31	1.48E-07	9,649	5,969	0,063	0,332	Boquita	Carrizales
lcl|TRINITY_DN45557_c0_g1_i3	Mucin-like protein	4.74	2.53E-07	6,015	5,033	0,241	0,195	Boquita	Carrizales
lcl|TRINITY_DN41123_c0_g1_i2	Tumor necrosis factor receptor superfamily member 16	2.99	5.34E-07	5,894	5,862	0,576	0,898	Boquita	Carrizales
lcl|TRINITY_DN41797_c1_g4_i1	Fucoxanthin-chlorophyll a-c binding protein A, chloroplastic	2.52	6.26E-07	54,061	53,145	8,53	10,02	Boquita	Carrizales
lcl|TRINITY_DN45766_c2_g2_i1	TNF receptor-associated factor 3	5.56	1.19E-06	255,566	152,843	1,654	7,034	Boquita	Carrizales
lcl|TRINITY_DN34963_c0_g5_i2	Voltage-dependent L-type calcium channel subunit alpha-1C	2.61	1.25E-06	5,211	6,857	0,9	1,073	Boquita	Carrizales
lcl|TRINITY_DN35616_c1_g3_i1	TRAF3-interacting protein 1	2.19	2.86E-06	9,157	9,753	1,706	2,459	Boquita	Carrizales
lcl|TRINITY_DN44060_c1_g4_i14	Amiloride-sensitive sodium channel subunit alpha	4.7	4.07E-06	5,231	3,901	0,178	0,176	Boquita	Carrizales
lcl|TRINITY_DN39128_c1_g1_i6	Radial spoke head protein 4 homolog A	4.98	5.65E-06	3,364	4,126	0,063	0,176	Boquita	Carrizales
lcl|TRINITY_DN45381_c2_g1_i2	Metal cation symporter ZIP14	4.83	7.49E-06	9,951	10,787	0,293	0,439	Boquita	Carrizales
lcl|TRINITY_DN29543_c0_g2_i1	Pumilio homolog 1	4.65	7.63E-06	5,101	4,018	0,126	0,244	Boquita	Carrizales

Continuation

Transcript ID	BlastP	log_2 (Fold Change)	P. adj.	Boquita brown	Boquita green	Carrizales brown	Carrizales green	Sample A	Sample B
lcl|TRINITY_DN58510_c0_g1_i1	Calcium/calmodulin-dependent protein kinase I	4.36	9.87E-06	5,332	7,081	0,157	0,449	Boquita	Carrizales
lcl|TRINITY_DN32048_c0_g1_i1	Sodium/calcium exchanger 3	3.76	1.35E-05	3,956	3,531	0,167	0,38	Boquita	Carrizales
lcl|TRINITY_DN38622_c2_g5_i1	Sodium channel protein	2.37	1.71E-05	6,969	8,427	1,13	1,844	Boquita	Carrizales
lcl|TRINITY_DN41319_c1_g1_i1	Caspase-8	3.97	1.27E-04	2,581	3,677	0,251	0,146	Boquita	Carrizales
lcl|TRINITY_DN45605_c2_g2_i1	Sodium bicarbonate cotransporter 3	2.95	3.30E-04	21,086	33,034	1,811	5,161	Boquita	Carrizales
lcl|TRINITY_DN42980_c0_g1_i2	Electrogenic sodium bicarbonate cotransporter 1	3	3.57E-04	9,619	11,177	1,622	0,956	Boquita	Carrizales
lcl|TRINITY_DN61984_c0_g1_i1	Protein dispatched homolog 1	3.84	1.03E-03	3,123	5,052	0,251	0,322	Boquita	Carrizales
lcl|TRINITY_DN41589_c0_g1_i1	Protein aardvark	6.73	1.10E-03	9,941	9,929	0,188	0	Boquita	Carrizales
lcl|TRINITY_DN23392_c0_g1_i1	Pullulanase 1, chloroplastic	4.12	1.17E-03	2,611	3,345	0,283	0,059	Boquita	Carrizales
lcl|TRINITY_DN42599_c0_g1_i1	Peroxynitrite isomerase THAP4	3.77	1.21E-03	4,288	3,238	0,136	0,41	Boquita	Carrizales
lcl|TRINITY_DN27464_c0_g1_i1	Magnesium transporter MgtE	-7.27	1.21E-03	0	0	3,998	3,483	Boquita	Carrizales
lcl|TRINITY_DN45538_c0_g5_i1	Atrial natriuretic peptide receptor 1	4.89	1.47E-03	5,462	2,702	0,188	0,088	Boquita	Carrizales
lcl|TRINITY_DN39313_c4_g1_i2	Fucoxanthin-chlorophyll a-c binding protein E, chloroplastic	3.72	1.65E-03	15,021	29,104	1,34	2,039	Boquita	Carrizales
lcl|TRINITY_DN70699_c0_g1_i1	Chaperone protein DnaJ 2	6.57	1.83E-03	2,591	2,643	0	0,059	Boquita	Carrizales
lcl|TRINITY_DN68415_c0_g1_i1	Mitogen-activated protein kinase kinase kinase A	3.5	1.94E-03	3,514	2,633	0,366	0,176	Boquita	Carrizales
lcl|TRINITY_DN30553_c0_g1_i1	Pyruvate, phosphate dikinase, chloroplastic	4.01	2.08E-03	3,183	3,735	0,073	0,351	Boquita	Carrizales
lcl|TRINITY_DN27957_c0_g3_i1	Potassium voltage-gated channel subfamily H member 7	4.02	2.33E-03	1,727	2,331	0,105	0,146	Boquita	Carrizales
lcl|TRINITY_DN23989_c0_g1_i3	Calmodulin	2.16	3.12E-03	3,133	2,897	0,513	0,829	Boquita	Carrizales
lcl|TRINITY_DN39799_c2_g1_i2	Neuropeptide SIFamide receptor	2.72	5.84E-03	4,669	2,497	0,607	0,488	Boquita	Carrizales
lcl|TRINITY_DN18789_c0_g1_i3	Peroxisomal membrane protein PMP34	-6.75	7.27E-03	0	0	2,439	2,898	Boquita	Carrizales